ORIG

Some corrections marked. Some New figures 8/18/88

SOME THEORY and EXPERIMENTS related to FRICTIONAL BEHAVIOR of ROCKS at LOW NORMAL STRESS

In revision for Pure and Applied Geophysics
(Submitted 8/25/86, accepted 9/86)
DRAFT: November 20, 1986
Several figures not finalised,
some quantitative information missing,
inadaquate reference to some works.

Andy Ruina
Theoretical and Applied Mechanics
Cornell University
Ithaca, NY 14853

Youval Katzman (2)
Aran Engineering
Mushav Ganot, Meshek 71
ISRAEL

Gerald Conrad (3)
U.S. Geological Survey
345 Middlefield Rd
Menlo Park, CA 94025

Franklin G. Horowitz (4)
Geological Sciences
Cornell University
Ithaca, NY 14853

ABSTRACT

Some theoretical questions related to slip on faults and in the laboratory are addressed: Spatially uniform slip is expected to be stable when slip is temporally stable and is likely unstable when slip is temporally unstable. Deformation in any gouge layer that has stick slip should not be smooth. Electronic control of effective machine-stiffness effects noise and stability. NONLIN Electronics

Results of several slip experiments with polished rock at low normal stress are presented: Step-change in slip-rate, with slip rates between .0001 and 100 μm/sec, reveals consistency with state-variable constitutive laws when short slip distances (<50μm) were measured close to the slip surfaces. A long slip-distance transient (≃ 100 μm) in friction stress was sometimes observed. The dependence of friction stress on steady-state velocity may be positive or negative for both virgin and run-in samples. At a step change in slip rate any surface separation is less than 0.1 μm. Step changes in normal stress at constant slip-rate lead to a transient in friction stress. The friction stress transient for nominally static friction experiments depends on the rate of slip before and after the nominally stationary contact. The stick-slip dynamics of the sandwich shear apparatus is more complex than that of a single degree-of-freedom spring-block system. About 100% of the work of friction is converted to heat. The coefficient of friction depends on apparently subtle variations in sample preparation and environment.

INTRODUCTION

The dynamics of fault slip depends in part on the frictional behavior of the potentially slipping fault surfaces. Of particular importance are slip- and/or slip-rate weakening, and strengthening during the nearly stationary contact which occurs between macroscopic slip events. These aspects of material response play a large role in determing the size, nature and even the existence of earthquakes if they are modelled as slip instabilities. The dependence of friction stress (shear traction) on normal stress and normal stress history is also important, in situations where normal stress may vary with position on the fault, distance slipped, or time.

Mechanical models of faults are implicitly based on the (possibly idealized) existence of a small region which includes a fault surface, shown schematically in figure 1, over which the stress is uniform and the deformation varies only in the direction perpendicular to the fault. This region, or continuum surface-point, interacts with the solid on either side by imposing a frictional boundary condition on the solid. This boundary condition is the constitutive law for the fault. Many constitutive laws that have been considered express relations between the time histories of the mechanical variables shown in figure 1: the slip distance δ, the shear traction τ (or friction coefficient $\mu \equiv \tau/\sigma$), the fault dilation δ_n, and the normal stress σ. In fact, most relations either ignore or treat as constant one or two of these variables. τ and δ are ignored in study of joint compression; σ is often assumed to be constant in friction tests; and δ_n, since it is often much smaller than relevant slip distances, is often well modelled as being zero.

The approach taken in these experiments largely follows from the work of Dieterich (1972, 1978, 1979, 1980, 1981). Dieterich observed 'time dependent' friction in nominally static friction tests, and also observed rate and history effects in sliding friction tests. The transient changes in friction stress that occur when the slip rate changes have also been investigated experimentally by Stesky (1975), Solberg and Byerlee (1977), Vaughan and Byerlee (1986), Dieterich and Conrad (1984, 1981), Ruina (1980), Tullis and Weeks (1986), Teufel (1983), Okubo and Dieterich (1984, 1986), Olsson (1986) and Teufel (unpublished).

Motivated by his experimental results, ideas about mechanisms for friction (as clearly enunciated in Dieterich and Conrad 1984), and earlier theories of metal friction (Rabinowicz 1958), Dieterich (1979) presented a state variable constitutive law. This law has since been generalized, modified to better fit real and imagined experiments, and changed to simplify the appearance of the equations (Dieterich 1980, 1981, 1986; Ruina 1980, 1983; Rice 1983; Rice and Ruina 1983; Tullis and Weeks (1986); and Rice and Tse (1986).

The possible applicability of these rate- and state-dependent friction laws has been studied by using them in models for slipping, primarily elastic, systems. Numerical models have been pursued by Dieterich (1979a, 1979b, 1980, 1986), Kosloff and Liu (1980), Ruina (1980, 1983), Gu et al (1984), Gu (1985?), Mavko (1983), Tse and Rice (1986), Rice and Tse (1986), and Horowitz and Ruina (1986). It has been found that certain details in the state-variable constitutive laws are of key importance in determining aspects of stability in slipping systems. Not suprisingly,

the stability related parameters in this model are closely associated with stability related parameters in cruder constitutive laws. Three such parameters are 1) the dependence of post-transient friction stress on rate of steady slipping; 2) the characteristic slip distance(s) in shear stress transients; and 3) the magnitudes of these transients. The degree of strength recovery or healing in stationary contact is also important, but does not have a simple analogue in at least some of the state variable descriptions (Ruina 1983).

The work presented here, which includes some previously unpublished results from Ruina (1980), was motivated by a desire to elucidate further some aspects of the constitutive law, especially by measuring transient effects with finer resolution.

The remainder of this paper is organized as follows:

First, general issues in the experimental design are discussed: homogeneity of slip and deformation, the effect of stiffness on noise and stability, and electronic control of effective stiffness.

Then some details of the experimental design are presented: the sample configuration, the load frame, slip and surface separation transducers, spherical air bearing mounting scheme, control circuitry, and miscellaneous experimental details.

Results from several types of experiments are then presented: Friction-stress transients at step changes in slip rate (both short- and long- slip distance observations); the effect of machine stiffness on step response; the friction transient at a step change in normal stress; the normal displacement at a step change in slip rate; the friction-stress transient and normal displacement after surface disruption; nominally time-dependent static friction tests, high-speed recording of stick-slip experiments; and comparison of mechanical work to heat generated.

Finally, three appendices address issues mentioned in the body of the text: 1) localisation of slip in the slip plane, 2) localisation of deformation in a fault gouge layer, and 3) a rate scaling rule.

GENERAL EXPERIMENTAL DESIGN CONSIDERATIONS

Continuum Point

If the purpose of a friction experiment is to reveal properties useful for continuum modelling, the sample should be such that its behavior approximates that of an imagined continuum point (figure 1). Thus, the slip, dilation and traction histories on all regions of the sample surface should be identical. A small sample is therefore attractive, since all points on such a sample have roughly the same velocity. However, the specimen must be large enough that a sufficient number of micro-contacts are included in the nominal contact region, making the response less subject to fluctuations from micro-scale inhomogeneity. The measurement

of surface 'point' properties also should be unaffected by the properties of the testing machine or of the adjoining bulk solid. It is not clear *a priori* that a sample meeting all of these conditions could exist, even in principle.

Most fundamentally, it is not clear that the concept of a continuum point can capture scaling properties of faults that may be relevant (e.g., Barton 1981). For example, characteristic lengths in material response may scale with sample size so that no unique characteristic lengths may be ascribed to the fault surface (See Ruina 1985 for a slightly longer discussion of this point.).

Uniformity of Slip

Even if the concept of a continuum point is sensible in principle, there is some difficulty meeting the condition of uniform traction and slip histories for several reasons:

1) The material involved in nominal contact changes in time: In most finite specimens different parts of the surface have different slip histories due to the material region of nominal contact changing in time. In the sandwich shear geometry of figure 3, for example, new surface is brought into contact at the top when the central rock slides down. This effect may not seriously contaminate data that is collected if *all* characteristic distances in material response are a small fraction of the sample length.

2) Rigid rotations of the sample about an axis normal to the slip surface cause a variation in slip rate: In the rotary shear geometry such gradients in slip are inevitable but are minimized by using a thin walled specimen, and by ensuring that the center of the sample is the center of rotation. Also, as explained in Tullis and Weeks (1986), if the effect of slip rate on friction stress is proportional to ln(slip rate), then neglecting slip displacement effects, the gradients in slip rate which occur in the rotary shear geometry have no effect on the measured form of the dependence of friction stress on rate.

3) Even for rigid samples, the loading geometry can be such that the desired uniform changes in shear stress would cause spatial variations in normal stress: In the sandwich shear geometry (figure 3), for example, an increase in friction stress (and vertical applied load) causes an increase in normal stress at the top of the samples. Placement of the copper shims (figure 3) close to the slip surfaces under the side samples reduces this effect. (The effect is from the moment caused by the separation of the friction force and the load point. It is proportional to the distance of the support points from the slip surfaces and can be made as small as the strength of the shims and rock allow).

4) Elastic deformability combined with sample asymmetry (i.e., the mechanical environments of all points on the surface are not identical) can cause non-uniform slip when there is a uniform change in shear stress (such a step change in shear stress is desired at a step change in the nominal slip rate). Similarly, asymmetry can cause non-uniform shear traction on the slip surfaces if there is an increase in applied load

while slipping is prevented.

The extent of this undesirable gradient in slip is roughly estimated by assuming uniform jumps in shear traction of the same size as changes in friction stress during the experiment. The formula below is justified by assuming linear elasticity and using dimensional consistency:

$$\Delta\delta = C(\Delta\tau)L/G \quad .$$

$\Delta\delta$ is the maximum difference in slip of two points on the surface, $\Delta\tau$ is a measure of the uniform jump in shear traction on the surface, L is a characteristic length in the sample (which depends on the sample geometry), G is an elastic modulus, and C is a proportionality constant which is on the order of 1. For an experiment to yield accurate measurements of stress change with slip, the stress change $\Delta\tau$ must take place during a slip displacement δ that is much larger than $\Delta\delta$ in the equation above. Otherwise, the details of transient stress changes will be blurred by the variation of slip through the sample.

Equivalently, in the cases where the transient involves slip weakening, the condition for uniform slip is that the sample is much smaller than the endzone (breakdown zone, Dugdale zone) that would be predicted for a shear fracture in an infinite medium (Rice 1983).

For the sandwich shear geometry the characteristic length L may be estimated, assuming $w \ll \ell$ (where ℓ is the length of the sample parallel to the slip direction, and w is the thickness of the sample perpendicular to the slip plane - see figure 3), by treating the side samples as elastic rods:

$$L = \ell^2/w \quad \Rightarrow \quad \Delta\delta \simeq (\Delta\tau)\,\ell^2/Gw$$

For a saw-cut triaxial sample, L=0 at the beginning of the test, before there is any offset between the samples, but it subsequently increases in a manner that depends on the details of the loading and jacketing constraints. For rotary shear samples with moderately thin contact region (compared to sample radius) L is approximately the thickness of the contact region. Related effects are discussed in great detail in Olsson (1987).

5) Similarly, elastic distortion combined with sample asymmetry can cause variations in the normal stress when there is a uniform variation in the shear stress. As is well known, however, for a linear elastic sample that is symmetric about the slip plane (but otherwise possibly inhomogeneous and anisotropic) the normal stress is unaffected by all distributions of slip on the surface.

6) Even if a sample has perfect symmetry, i.e. all points on the slip surface are identical to all others in all properties and loading, uniform slip is not ensured. Uniform slip could be unstable to small spatial perturbations, thus leading to spatially non-uniform slip. However, it

appears generally true that the conditions for the onset of spatial instability from uniform slip are generally met *after* the conditions for temporal instability. Thus, a nominally uniform sample which is far from stick-slip is also a sample with no regions of localized slip. This result is roughly rationalized in Appendix 1.

The above reasoning does not bar the possibility that a friction law observed macroscopically to be smooth could be an average of 1) many microscopic unstable jerky motions which, separately, do not have a simple continuum description, or 2) spatially localized slip motions governed by a different continuum constitutive law than that macroscopically observed (Appendix 1).

Uniformity of Gouge Deformation

Slip on faults is often associated with a layer of fine particles or gouge. In friction experiments such a layer is sometimes introduced artificially. Even if not introduced artificially, particles are probably always generated by slip.

Frictional fault constitutive relations, when first proposed by Dieterich (1979), were reasonably suggested to express relations between strain γ in a gouge layer and shear stress. When Dieterich (1981) presented his experiments with gouge layers, however, he was careful to express his measure of deformation as displacement δ.

Roughly three cases can be distinguished in terms of gouge deformation:

1) the deformation is homogeneous in the gouge layer and the gouge may be treated as a continuum with shear strain $\gamma=\delta/h$ (where h is the gouge layer thickness). For a given stress, total apparent deformation should be proportional to layer thickness.

2) The deformation is confined to one narrow slipping layer whose internal structure is not well defined as a continuum. In this case slip δ is the sensible deformation measure. For given stress history, total apparent deformation is independent of layer thickness.

3) Deformation takes place through the thickness but with spatial structure over the length scale of the layer thickness. In this case slip might be well defined on some internal surfaces and deformation well defined on other surfaces, but the regions are too large too be reasonably averaged as a continuum. It is not clear how deformation should scale with thickness. In this case the slip δ is the sensible deformation variable but it is associated with the particular gouge layer at that thickness - not the gouge material alone and also not the wall surfaces alone.

The experimental observations of gouge layers (eg. Dieterich 1981), the location of many aftershocks on nearly planar surfaces, field observations of exposed faults (Weldon and Sieh 1985), and the theory in Appendix II support the following claim: Neither laboratory stick-slip nor real

earthquakes can be described adequately by a homogeneous continuum deformation of a gouge (or fault zone) layer. Any gouge (or fault zone) layer that is said to predict the details of stick-slip instabilities and/or earthquakes cannot be fully characterized by its continuum deformation properties. Localization of deformation to a surface, to surfaces, or to some kind of dis-continuum flow, necesarily precedes or coexists with the elastic instability.

Experiments aimed at explaining friction-elastic instabilities should, in general, acknowledge that the overall gouge layer and its side boundaries are the object of study, not the material in the layer (unless, of course, it is the prediction of layer properties from material properties that is the object of study).

Stiffness, Servo-control, Instability and Noise

Neglecting inertia, a testing machine may be characterized for some purposes by an effective stiffness K_{eff} which effects the dynamics of slip, the measured signal and the noise in measurement. K_{eff} relates the sample load to the sample inelastic deformation when the load point (the point on the testing machine where deformation is controlled) is held constant.

Force or friction coefficient might be used as a measure of load, and average sample strain might be a useful measure of slip some purposes. But for slip experiments, friction stress and slip displacement seem to be natural measures with which to scale stiffness. In these terms the load

point displacement $\delta_{\text{load point}}$ can be related to sample load τ, and slip δ by the effective stiffness K_{eff} as:

$$\delta_{\text{load point}} = \delta + \tau/K_{eff}$$

For example, nominal slip may be imposed on on sample by imposing a definite actuator motion (δ_t in figure 4). In this case the full compliance of the machine (springs K_s and K_m in series in figure 4) determines the load drop if the sample slips more than the nominal slip.

If, on the other hand, transducer signal δ_s is controlled as the load point, the sample feels only the compliance of the material between the sample and the transducer mounts, and the effective stiffness.

Thus one may think of a standard servo-controlled machine used in displacement control (δ_s controlled) as being artificially stiff. That is, if the servo-control works well and much faster than the time scales of interest in material response, the machine moves in such a way the measuring transducer reads what the reference signal commands independent of sample deformation. The closer are the transducer mounts to the deforming sample, the closer the effective load point is to the sample and the stiffer appears the machine.

It is also possible to vary the effective position of the transducer mounts and thus the effective machine stiffness. This is because the machine is approximately linear elastic and all relative elastic displacements are proportional to the load. The stiffness of the machine is increased by subtracting some of the measured load signal from the measured displacement signal. The stiffness is decreased by adding some of the load signal to the measured displacement signal.

$$\delta_{\text{load point}} = \delta_s + C\tau = \delta + \tau[1 + CK_s]/K_s$$

Here δ_s is the measured slip displacement, τ is the frictional stress, and K_s is the nominal stiffness bof the sample (the stiffness between displacement-transducer mounts). C is the gain of an amplifier which multiplies the load signal before it is added to the displacement signal (it has units of inverse stiffness). So, for the three cases that have been described, the effective stiffness K_{eff} is given by:

$1/K^{eff} = 1/K_s + 1/K_m$ with no servo control

$K_{eff} = K_s$ with simple servocontrol

$1/K_{eff} = 1/K_s + C$ with electronically controlled stiffnes s

A finite negative gain C on the stiffness controlling amplifier can provide infinite stiffness (zero compliance), while an infinite positive C leads to zero stiffness (infinite compliance).

An electronically-variable effective stiffness (as provided by the variable gain C) is not standard equipment on commercial testing machines (we would appreciate hearing of any users of this technique in material testing). We originally added it to our circuitry for the purposes 1) of making the machine more stiff, and 2) for checking the effect of stiffness on slip stability. In practice, however, we mostly used the circuit to decrease the machine slightly stiffness so as to diminish the effects of electronic noise.

The jaggedness of friction-stress traces, or what loosely might be called noise (see figure 9) is intametely linked to machine stiffness.

1) Electrical noise has both obvious direct and more subtle indirect effects. The indirect effects come from the experiment being sevo-controlled so that electrical noise causes actual variations in the load on the sample. The effect of electronic drift (the low frequency part of this noise), which may come from temperature fluctuations in the transducer and transducer circuitry, is explained below.

Assuming the inelastic deformation of the sample is negligible over the time period of the noise, the fluctuation in load due to noise is given by:

$$\text{Fluctuation in load} = (\text{effective stiffness}) \cdot (\text{displacement noise}).$$

Thus, servo-control with the transducer mounted very close to the deforming surface, and similarly the use of artificial stiffness as described above, can only be useful to the extent that the measurement of displacement has little noise, drift, or slop (small-cycle hysteresis). An infinitely stiff machine produces an infinitely noisy load.

2) The rate of electronic drift produces a perturbation of the nominal slip rate. Its effect is exascerbated at smaller slip rates (since inelastic samples typically have a weaker than linear dependence on rate). The effect of perturbations of nominal slip rate are reduced by increased effective compliance.

3) For higher-frequency electronic noise, such as the perturbation from steady ramping in the reference signal due to stepping of the digital-to-analogue converter, load fluctuations of the type being discussed here are not diminished by increased slip rate. This is because high speed changes in the reference signal lead to high speed changes in the sample displacement and load. So greater machine compliance still reduces the effect of this higher frequency noise. If the frequency of the noise is much higher than the response frequency of the servo controlling system (and is not such large amplitude as to saturate any of the amplifiers), the noise effects are reduced to simple noise in the data.

4) Another source of "noise" is instability. While some point in the machine system, the so called load point, may be directed to move at a nominally constant rate, steady sliding may be unstable. The instability may be the result of interaction of the slip surface with the elastic system. Or it may be that the load point is imperfectly controlled and that the instability involves the dynamics of the whole control system as well as the slip surface.

It seems to be true that, at high effective stiffness, high slip rates lead to control instabilities. This might be rationalized roughly as follows: At high stiffness, fluctuations in nominal slip displacement or nominal slip rate are associated with a shear stress transient with a short characteristic distance. This characteristic distance is a property of the sample. Because the testing machine is compliant, the actuator must have large fluctuations in rate in order to maintain constant rate at the effective load point. As slip rate is increased the speed of response for this fluctuation increases to a point where it is beyond control.

Instability may or may not be easy to detect: Clear relaxation type (sawtooth) oscillations, likely to be largely elastic-friction instabilities, can sometimes be detected if the friction stress traces are examined in detail. High-frequency (in the kiloherz range) control instabilities can sometimes be observed with an oscilloscope, or detected by auidible sound. Very large control instabilities involving disruption, and sometimes damage, of the sample can be easily detected by all instruments as well as sound, sight and feel.

The following rules of thumb apply to simple servo-control systems of the type described here. High gain in the feedback amplifier promotes control instabilities, while low gain leads to poor experimental control (slow system response). High stiffness enhances control instabilities and noise in the load, while low stiffness leads to frictional instabilities. Also, at high stiffness, control instabilities appear at high slip rates.

A goal of friction experiments, at least in the context of earthquake prediction, is to measure frictional properties that are associated with instability. In order to measure these properties one wants the experimental system to be stable. Such stability can be achieved, in some circumstances, by mechanical means such as high physical stiffness. In the experiments here we have tried to obtain stability through use of electronic control. This approach has the drawback that new sources of noise and instability are thus introduced.

Quantitative stability analysis of the controlled system might be fruitful. However, our experience has been that important, even first order, effects seem to be essentially non-linear (because of friction) and thus may not yield easily to formal analysis. Some of the results of our intuitive non-linear analysis are indicated in the description of the control circuitry below.

EXPERIMENTAL METHOD for Rotary Shear and Sandwich Tests

The recent experiments were conducted in a servo-controlled "tension-torsion" load frame using cylindrical samples in a moderately dry- or room-air environment. The samples (figure 2a) were connected to small local slip- and normal-displacment transducers (figure 2b) and mounted in a special fixture (figure 2c) connected to the load frame (figure 2d). The servo-controlled quantities were the normal load and some measure of the slip displacement.

The earlier experiments from Ruina (1980) were performed in a normal room environment in the sandwich-shear (figure 3) apparatus of Dieterich (1979) (slightly modified).

Since the sample, transducers, load frame and electronics for both of these experiments are not quite standard they will be discussed in some detail below.

Samples

Some of the rotary-shear samples were cut from 1 in diameter cores of Arkansas Navaculite, a very fine grained pure quartzite, the others from Eureka Quartzite. The geometry of the slip surfaces is shown in figure 2a. Only a strip of .06 in width is involved in the sliding contact. The indentation in the upper sample is exaggerated in the figure. The samples were shaped with a water-lubricated diamond grinding wheel while collet-mounted in a lathe. The samples were then mated by being ground together about 5 to 20 quarter revolutions, mounted in the load frame as during an experiment, with #90 grinding grit and water. After mating, the

samples were rinsed with water and dried in place. Data collection was sometimes begun at this point, and otherwise after the samples had been slid against each other some distance and had generated small amounts of gouge - visible as a dusting of white powder.

The sandwich shear samples were cut from Eureka Quartzite in the geometry shown in figure 3. They were shaped with a grinding machine and then briefly lapped by hand (only 5-10 strokes to prevent change in the overall surface shape) with #90 grit grinding compound and water.

Load Frame

The load frame for the rotary shear tests is an INSTRON-1321 two post tension-torsion frame rated for 20,000lbs (90,000N) and 10,000 in lbs (1100 Nm). It is shown in perspective in figure 2d. The actuator shaft is connected at its top to the collet assembly for the lower sample (figure 2c). It passes through the axial actuator (with a ring piston inside the actuator) and holds up the rotary actuator and a sliding cross head, both of which move up and down with the actuator shaft.

In the two post design, the torsional rigidity of the frame comes from the torsional and bending rigidity of the two (long) posts. The frame is therefore fairly compliant in torsion. The RVDT measurement consequently includes an undesirably large amount of machine distortion. This distortion does more than just increase the effective compliance of the servo-controlled machine. For very small angles of actuator rotation and zero normal load, the net effect of a small rotation was zero slip, and

sometimes even a small reverse slip. These effects werely possibly due to rotary friction in the axial actuator, leading to a distortion of the load frame.

Figure 2d shows a space truss that we constructed in order to minimize the reverse slip just mentioned. The frame is constructed of welded 1 inch square steel rods. The truss, which includes the verticle posts of the original load frame, is statically determinate (if modelled as a pin jointed structure) for all loading modes (except one, which cannot be applied by the attached actuators). By design, and as verified by measurement, the added trusswork increases the load frame's torsional stiffness by a factor of about 50.

Transducer Design and Placement

Slip displacement was sometimes measured with an LVDT (linear variable displacement transducer) in the sandwich tests, or an RVDT (rotary variable displacement transducer) in the rotary shear tests. The mounts for these transducers were removed from the slip surfaces. In many experiments slip was measured with a small transducer mounted close to the slip surface. In some of the rotary shear experiments, normal displacement was also measured close to the slip surfaces. In all cases shear and normal load was measured with commercial load cells.

Fine-resolution slip displacement is measured by the bending of a thin cantilever beam (.005 in ≃ 125μm thick stainless steel shim-stock, ~~about~~ the cantilever assembly is connected to a fixture attached to one sample (the lower sample in figure 2b, the middle rock in figure 3). The cantilever is bent by the tip of a pin attached to the other sample. The full range of the cantilever transducer in the geometry we used was 30 - 200 μm. The semiconductor strain gauges are light- and temperature-sensitive so in the rotary shear experiments the load cells, sample and collets were all enclosed in an insulated box into which air from the air bearing (described below) was constantly flowing. Over a time scale of hours the measured displacement of an unloaded (and presumably non-slipping) sample would drift by up to about $\pm$0.1μm. Over a period of several seconds it would drift up to $\pm$0.02μm.

In some of the rotary shear experiments, normal displacement was measured with a capacitor, one plate attached to each sample (as shown in figure 2b). Each plat has the shape of an annulus, with inner radius just larger than the sample and width of about 5mm. For alignment the plates are separated by a heavy piece of paper when the samples are brought in contact and the transducers are clamped to the samples. The paper is removed to permit measurement. An AC bridge circuit is used to convert the capacitance to a voltage which is a nonlinear function of separation distance.

To the extent that the capacitor plates are not perpendicular to the rotation axis, large sample rotations lead to non-parallel plates and a measured signal which does not correspond to actual sample dilation. Severe misalignment can even lead to plate contact. We were only interested in the normal displacement occuring in very small rotations (corresponding to transients of short slip duration $\simeq 10\mu m$), however, so that the slow variation in capacitor reading due to imperfect capacitor alignment was not important. The capacitor was calibrated by cross-plotting its reading against that of the Instron LVDT (see figure 2d) as the samples were brought into contact. The tangent of this curve when the surfaces made contact was used to calculate the scale factor for the approximately linear response of the capacitor transducer. The capacitor had a resolution of about $0.1\mu m$ in our arrangement.

In all of the experiments the local transducers are held in place by fixtures which are clamped about 5mm from the slip surfaces.

The rotary and axial load cells are supported from above by the upper cross member of the load frame, and below they support the collet for the upper sample. The commercial load cells used had ranges of 500 lbs ($\simeq$2200N) and 1000 in lbs ($\simeq$110Nm). For practical reasons, the stack of load cells included others which were not being used, and thus formed a support for the upper sample with undesirably large lateral compliance. As described below, the net lateral friction force had to be held near zero to prevent misalignment. Construction of a lateral constraint, compliant in torsion and extension (so as not to effect the load readings) was considered but not undertaken.

Sample Mounting

Early experiments in the rotary shear apparatus revealed some problems with simply clamping the lower sample to the actuator shaft and the upper sample to the load cells:

1) The samples sometimes did not wear uniformly.

2) When the direction of rotation was reversed, the samples would often shift their relative horizontal positions by a slightly visible amount, perhaps .2 -.5 mm, thus shifting the center of rotation. The motion is apparently due to horizontal forces generated by non-uniformities in the friction stress, acting on the lateral compliance of the load cells. Assuming a uniform coefficient of friction, this must be due to a eccentric normal stress resultant. For a thin circular ring of contact being rotated about its center, the lateral force vanishes when the centroid of the normal force is the center of the circle (In which case moment balance of the normal forces about the ring center implies that the horizontal friction force resultant equals zero).

3) The testing machine is relatively stiff in the axial direction, as are the samples. The MOOG actuator valves are essentially flow control valves, so small fluctuations in the signal sent to the axial actuator could cause large load variations. This high machine stiffness expresses itself in inadaquate load control leading sometimes to accidental fracture of the samples. Such stiffness effects are discussed in the text with regard to slip motions.

We designed a clamping arrangement that seemingly overcomes the difficulties just named while maintaining high torsional stiffness. The support ensures that the resultant of the normal stresses on the slip surface is a vertical force at the center of the contact ring.

In this arrangement the lower sample is held against the upper sample by a spherical air bearing (as suggested by Garwin (1984)) and some torque straps as shown in figure 2c. The center of the sphere is the center of the circle of frictional contact and is stiffly held on the axis of rotation by "torque staps". The torque straps connect a bucket which is rigidly attached to the actuator shaft to a bucket which is rigidly attached to the lower sample. The straps are thin sheets of metal in the plane of contact between the two samples. The net effect of this geometry is to make the lower sample stiff for horizontal displacements (stretch of the torque straps); compliant for vertical displacement (bending of the torque straps and reduction of the air gap in the bearing); stiff for rotation about the sample axis (stretch of the torque straps), the motion involved in slip; and compliant for rotations about horizontal axes that go through the center of the circle of contact (bending of the torque straps).

In some of the experiments, air to the air bearing had water and air drops filtered out in a condensing tank at high pressure (80 psi). The air was consequently extremely dry (10% or less relative humidity) when released from the bearing at atmospheric pressure. Because the sample was enclosed, this air dominated the sample environment and may effect the observed results as might be expected from the experiments of Dieterich

and Conrad (1984). In the sandwich shear experiments, the samples are mounted in the apparatus of Dieterich (1979) and mounted as shown in figure 3. As explained above, the thin copper shims mounted close to the slip surface are used to minimize the moment of the support force about any line in the slip surface.

Control Circuitry, Artificial Stiffness

The control circuitry used in sample rotation, along with an idealisation of the testing machine, is shown in figure 4. A reference signal is provided by a 14 bit (12 bits used in the sandwich shear tests) computer-controlled digital to analogue converter. This reference signal is ramped in time at various rates to cause nominally constant slip rate motions. The reference signal is compared to a feedback signal from the transducers, and the difference is used to control a MOOG valve connected to the rotary actuator.

Because we were interested in fast response for very small motions (.01 μm $\Rightarrow$ 1 μradian), smaller perhaps than a standard testing machine is designed for, we needed a high gain to overcome (non-linear) friction and internal leakage in the actuators. On the other hand high gain tended to cause large control instabilities. In other words, while the machine was stable to small perturbations (and even slow in response), it was unstable to large perturbations. Occassional electronic noise or steps in control signals are inevitable, so that it is not practical to operate the machine in a control regime where small perturbations decay but where large vibration instabilities can be excited.

In order to have high gain for small signals (for fast response) but low gain for large signals (to prevent large-amplitude vibrations) we constructed a non-linear amplifier to power the MOOG valve. The circuit provided a monotonic relation - three linear segments - between control error (input) and valve current (output), such that it had high gain for small signals, but ultimately saturated in order to limit the maximum current to the MOOG valve. This last clipping circuit is functionally equivalent to a flow-limiting valve on the actuator. The resulting circuitry permitted fast machine response ($\simeq$.03 sec) for very small signals (0.0005^{o} rotation $\simeq$.01 μm slip using the cantilever displacement transducer) while effectively preventing any finite amplitude control instabilities.

After an internal leak in the rotary actuator was discovered and repaired it was found that the high gain for small signals in the feedback circuit was less important in improving response, however.

In general, the evolution of the apparatus has been aimed towards a reduction in noise of the various kinds discussed previously. At any rate, any inferences made from observations of the visible fluctuations need to take account their source, which is not just the slip surface.

Further Miscellaneous Details

Some technical details are mentioned here for other researchers who may use, or intend to use, equipment similar to our own.

Electronic noise in our system was substantially reduced by adding heavy independent ground wires to all controlling amplifiers and their enclosures. Development of the control systems was greatly aided by use of a six channel panel meter and a storage oscilloscope during all tests. The LVDT on the Instron machine, which might have been used to measure surface dilation, also measures the deformation and slip dilation of the rotary actuator seals. A change of hydraulic fluid, as suggested by Instron, had a large positive effect on the rotary response of the load frame for small signals.

The testing machine we used was oversized for our purposes, as the maximum torque we measured was 1/200 of the range of the machine. Though one cannot simply say why it should be so, and it might not be true, it *seems* that the size of the machine contributed somewhat to the difficulty of controlling the fine motions we were studying.

The samples we used would occasionally chip. The upper ground surface should, preferably, have been ground so the the ridge of contact was somewhat indented from the outer radius. This way the contact stresses (which have a tensile component for high coefficients of friction) would be born by a larger support foundation, and there would be no sharp corners near the contact region.

RESULTS

The data we present was collected over a period of years (1978-1985) when the equipment described above was in various phases of development and repair. Hundreds of tests were performed. Most of these, however, were designed to reveal, or accidentally served to reveal, some defect in the experimental apparatus or procedure. Thus many results presented below are not associated with a desirable amount of systematic control of relevant parameters.

Short Distance Transients at Step Change in Slip Rate

Much recent work in rock friction is based on observations during an experiment in which a step change in the slip rate is imposed on the slip surface. In our case we kept the normal load constant during such steps. Results from the sandwich shear apparatus which were also shown in Ruina (1980) are shown in figure 5a with the results of a similar experiment for rotary shear in figure 5b. In both cases: the samples were Eureka quartzite, had been ground with #90 grit abrasive, had undergone substantial slip before the data was collected, and were in an open room environment (unknown relative humidity).

The central observation is that the friction force makes a step increase at an increase in slip rate and then decays in a decreasing manner to a new level (The words 'increase' and 'decrease' can be interchanged.). The decay is very quick at first and then seems to follow an exponential decay. The primary difference to note between the figures 5a and 5b is in the sharpness of the initial rise and decay. This is apparently because slip in the rotary shear apparatus is more homogeneous than in the sandwich shear apparatus.

In fact, the homogeneity of slip was explicitly checked in some of the sandwich shear experiments by mounting a second displacement transducer at the back lower left corner of the samples (the first tranducer is at the front upper right) and then comparing the response of the second (not servo-controlled) transducer to the response of the first contolled transducer. A difference of up to *.*μm was found when the load rate was changed.

Figure 6 shows the largest range of slip rates that were performed with a single sample (10^{-4}-$10^{2}$$\mu$m/sec - for comparison, typical average relative tectonic plate motion is about 10^{-3} μm/sec). The higher rate experiments were performed using the RVDT for a displacement transducer. In this range of speeds both the frictional increase with step in slip rate and the eventual decay appear to be roughly independent of slip rate. At the highest rate (100μm/sec) the initial peak appears noticibly lower. But this has no meaning since neither the machine nor the plotter could accurately control or record a transient of such short duration ($\simeq$0.01 seconds).

The inferred values of the parameters A, A-B and C are indicated in the figures. The parameter C (for *confusion*?!) proposed by Dieterich (1981) (and called 'B' therein) and also used in Vaughan and Byerlee (1986) and Lockner and Byerlee (1986) which is (correcting a sign error from the first two of these papers)):

$$C \equiv \Delta\mu / log_{10}[(V_{\text{new steady state}})/(V_{\text{old steady state}})]$$

In order to simply relate the data to certain constitutive laws Tse and Rice define the parameters A/σ and $(A-B)/\sigma$ by:

$$\begin{array}{lll} A/\sigma & = \left\{\partial\mu/\partial(\ln V)\right\}_{\text{instantaneous}} & \text{at constant } \sigma \\ (A-B)/\sigma & = \left\{d\mu/d(\ln V)\right\}_{\text{steady state}} & \text{at constant } \sigma \end{array}$$

where $(A-B)/\sigma \simeq .43 \cdot C$.

A, B and C may depend on slip rate V as well as all conceivable material and environmental factors. Interpreted in terms of a specified constitutive law A, B and C can be found from parameters in that law. For example $A/\sigma = a$ and $B/\sigma = \sum b_i$ for the a and b_i used in Weeks and Tullis (1985).

The values of A and A-B (or C) may be inferred quite directly from experimental data for step changes in slip rate at constant normal stress if a few conditions are met: 1) The testing machine is sufficiently stiff so that the direct rate dependence (if that is in fact the correct idealization for the constitutive law) can be accurately inferred, 2) that after the step change in slip rate the friction stress does in fact approach a steady state value.

Some of the details of the shape of the transient in shear stress at step change in slip rate change from experiment to experiment for both explicable and currently inexplicable reasons. Several examples are shown in figure 7. All of these examples are from the rotary shear apparatus - at various stages of development.

Speculations and conclusions based on the above data are as follows:

1) The short distance transient, visible in figure 5a and also in some of figures 7, consists of a peak and a decay of the same approximate magnitude. This short distance peak may in fact be well less than .25 μm and may, for some purposes, better be described as a direct dependence on acceleration. That is, the mathematical description of the transient can be shown to approach the response of a direct dependence on acceleration in the limit of slow variations in slip rate (Ruina 1983). If so, the effect of the short distance transient in linear stability analysis is the same as the effect of inertia (see Rice and Ruina 1983).

2) The steady-state dependence of friction on rate may be positive ($C>0$) or negative ($C<0$). In particular, a negative C is observed in some experiments starting with virgin samples. Thus the suggestion of Dieterich (1981), in reference to figure 8 therein, that the observation of negative steady state rate dependence ($C<0$) depends on substantial slip, was satisfied for some but not all of our surfaces. For some surfaces C was less than zero from the start. The differences in procedure or environment that separate these two cases

is not known.

Variation in Shear Traction for Large Slip Distance

The observations above are centered around experiments in which short distance transients were recorded. In some experiments controlled with an LVDT (sandwich tests) or RVDT (rotary shear tests), transients in friction stress due to step changes in rate were recorded over much longer distances. There was sometimes, but not always, observed to be a transient with a much longer decay distance (on the order of 100 μm) than those observed above. This long distance transient is of the opposite sign from what is assumed for transients in Ruina (1983) and Rice and Ruina (1983) but seems to be similar to that observed in Dolomite by Weeks and Tullis (1985). Again we do not know what changes in environment or procedure cause the appearance or disappearance of this effect.

Figure 8a shows the results for a sandwich specimen. Figure 8b shows results for a rotary shear specimen. Figure 8c shows results for a rotary shear specimen where the long distance transient was not observed.

Effect of Stiffness on Step Response

Figure 9 shows the effect of stiffness on the nature of the response in shear stress to a nominally static friction test. At high stiffness there is a sharp response (and substantial noise as discussed earlier). At lower stiffness the response is less sharp. At still lower stiffness instabilities of the type discussed in modelling papers such as Gu et al (1984) start to become apparent.

Similar observations were made on the rotary shear apparatus but not with as large a range of stiffness.

Step Changes in Normal Stress During Steady Slip

Figure 10 shows the shear stress when a step change was made in the normal stress at constant slip rate. The step in normal stress was actually a ramp spread out over 0.5 seconds so that the servo-control system could keep up with any consequent variations in load. In 0.5 seconds the accumulated slip is only 0.05 μm so that, relative to the longer of the short characteristic slip distances of the surface, the step change may be regarded as instantaneous.

Experiments of this general type have been reported by Olsson (1985,1987) where the observations were similar to those of figure 10 here. Olsson's experiments were different in some detail (he stopped slip while stepping the normal stress) but the data he collected look similar.

A few observations may be made about these experiments. One is that the transients are relatively simple compared to the transients associated with step change in slip rate. The other is that they seem to be essentially non-symmetric for increased and decreased load. This assymetry cannot in general be described by any linearized description of the type proposed by Olsson (1984, 1987) as an analogy to the linearized description in Rice and Ruina (1983) for effects of slip rate history. If , however, only monotonic increases or decreases in load are assured in the slip history then only the step up or only the step down data might be used in the description. Such monotonic loading can occur in a linearized description of instability if the eigenvalues in the characteristic equation are real. How well this assymetry would be maintained for smaller load steps is unclear.

The memory effects associated with normal stress changes, at least as indicated here, do not seem particularly important and might be sensibly neglected in normal stress analysis.

Unfortunately we did not monitor the normal displacement at the time of these experiments.

>Normal Displacement

Tolstoi (1957) has claimed that normal displacements play an essential role in characterizing the friction force. Experiments by Sakamoto, Tanii and Tsukizoe (1980) were also aimed at measuring normal displacement in slip. Both of these experiments were with metals.

Within the resolution of our transducer ($\simeq 0.1\mu m$) we were unable to measure a normal displacement when the slip rate was changed by a factor of 10 in the slip speed range of .001 to 1 μm/sec. Thus any normal displacement effects associated with frictional transients and their associated change of state must be of size 0.1 μm or less. We could have increased the sensitivity of our surface separation measurement by decreasing the capacitor gap.

We did not attempt to measure surface dilation associated with the long distance transients described above.

In contrast, we did notice a normal displacement effect when the sample was disturbed in a major way such as with a control instability. Approximately 5 observations were all consistent with the following: When constant rate slip is resumed after a major disturbance, there is a transient in shear stress that has a greater distance associated with it than the short transients. This transient may involve a relaxation from above or from below the ultimate stress level for steady sliding (see figure 11). If the stress relaxed from above, the surfaces were compacted during the disturbance (as measured by the capacitor). If the stress rose from below the gap dilated during the disturbance.

This behavior is exactly of type observed for dry soils. If they are tightly packed they dilate and soften with ongoing shear. If they are loosely packed the compact and harden with ongoing shear.

It is possible that the long distance stress transients we observed at step changes in slip rate would be associated with similar normal displacements as those noted above, and for similar reasons, but we have no data to check this idea.

Time-Dependent Static Friction

Only one systematic test was made on time dependent nominally static friction. The tests are called 'nominally static' because only the load point speed is stopped, whereas the samples may continue to slip. Such continued slip is observed by a slow drop in load and is also predicted by some sonstitutive laws.

An experiment in rotary shear was performed in which the nominal slip rate was V_o as controlled by the RVDT. The load point was then stopped for time t_o and finally slip was resumed at speed V_o. An example of friction stress vs. nominal displacement is shown in figure 12a. The results of this experiment are summarized in figure 12b. As in Johnson (1981) the jump in shear stress is plotted vs $v_o t_o$. The near-collapse of the data when plotted with such an axis is itself a statement about the constitutive law for frictional slip (see Appendix III).

Heat Generated During Slip

One set of tests in the sandwich apparatus was designed to check some aspects of the energy budget. In particular: does frictional work equal heat or is a noticable amount of energy spent on surface energy of new surfaces (on gouge paricles), strain energy of deformed near surface material, or high-frequency acoustic radiation.

The test was designed so that we did not need to depend on the thermal properties of the rock or on the solution of partial differential equations. A side rock in the sandwich apparatus was prepared with 4 thermisters mounted inside the rock (drilled in from the back) near the slip surface. The thermal pulse, from sliding at a fixed rate for 30 seconds with a measured load, was recorded. The load is nearly constant during the pulse so the mechanical work rate is also nearly constant.

The thermal pulse is compared to that from electric heating. A thin sheet of metal is mounted between the same rocks as in the friction test and a current is passed through. The voltage and current are both measured during an electrical pulse that has a constant power for 30 seconds.

Figure 13a shows a thermal pulse for frictional sliding as compared to the pulse for electrical work in figure 13b.

Unfortunately, there was thermal drift in our apparatus (several milli-degrees) so that comparison was not very accurate. In the most careful of test runs (for a set of 12 pairs of measurement) the temperature pulse generated by mechanical work was 99%± 6% of the temperature pulse for the corresponding electrical work (taking account both the statistical and expected systematic errors).

Taking all of our data into account, however, the best we can say is that about 90%±20% of the mechanical work goes to heat.

High Speed Measurement of Stick Slip

Neglecting inertia, a complex testing machine with a sample, consisting of many heterogeneous elastic parts, is well modelled, and in some sense precisely modelled, as a single degree-of-freedom spring block system. The simplest dyanamic analysis of stick-slip which include inertia also use a single-degree-of freedom model. However the dynamic analysis is based on the model that the two halves of the specimen are point masses.

We used the high speed recording apparatus of Dieterich (1979b) and Okubo and Dieterich (1986) to moniter stick slip in the sandwich apparatus of Dieterich (1979a). The experiment was not servo-controlled, but slip displacement was measured with a cantilever transducer and stress was moniterred with a strain gauge on the surface of the rock near the cantilever.

During stick-slip it was found that, following an initial transient of the general form of figure 7, that slip motion was stopped, apparently by a "reflection" off an internal machine component. Such reflections also stop the slip in the large apparatus of Dieterich. In the sandwich tests it was found, however, that slip then resumed and stopped once again. That is, that what appears to be simple stick-slip when recorded over a time scale of $\simeq$ 0.1 seconds is really a combination of two slip events. Figure 14 shows a typical result. What is plotted as shear stress τ is actually the shear strain as measured close to the displacement transducer.

Such a result should not be particularly suprising since the testing machine does not resemble either a massless spring (classical stick slip), or a homogeneous elastic layer with a simple boundary condition.

CONCLUSIONS

The material response to all transient experiments was quite repeatable, at least in quality. However the overall level of the coefficient of friction was highly variable. Humidity (as discussed in Conrad and Dieterich (1984)) might be a significant uncontrolled variable. It seems however that other uncontrolled aspects of the material preparation and use were also important.

Despite considerable variability in the coefficient of friction from month to month, day to day, and even within a friction experiment, some aspects of the frictional behavior were universally observed. In particular, at a step increase in slip rate the friction stress makes a step increase and then decreases over a short distance (approx 10 μm). This single aspect of the frictional behavior is sufficient to explain many observed phenomena as has been explained in the many modeling papers mentioned previously.

However, at least in the experiments performed here, there is a large variation in the overall coefficient of friction that is not well explained by the constitutive laws which describe the short distance transients described above. It seems likely that environmental effects of the general type studied directly by Dieterich and Conrad (1984) are significant. The extent to which these variations need to be understood for useful geophysical modeling is unclear.

APPENDIX I: Localization of Slip Along the Slip Surface

Localised slip refers to inhomogeneous slip on an esatblished slip surface - in contrast to localized deformation (to be discussed later) which refers to localisation of deformation to slip on a surface. The paragraphs that follow are an extension of an argument put forward by Dieterich (1979) and also in Rice (1983). Dieterich motivated use of large samples in his earthquake simulations (as opposed to his sandwich shear friction experiments) by the claim that large samples were needed for a slip event to remain confined within a sample. Rice pointed out that a sample that was not large enough to contain the endzone for an imagined fracture was a sample in which uniform slip could be expected. Confined slip events and propagating slip rupture are the two primary examples of what is meant by localised slip, but more complex patterns of inhomogeneous slip are also meant to be included in the concept.

Restated, the claim is roughly this: Any sample that is capable of slip localised along the fault surface is also capable of temporal (stick-slip) instabilities.

The result is justified by comparing the conditions for temporal instability to the conditions for: 1) stability to spatial perturbations from homogeneous slip, 2) the existance of a propagating shear fracture, 3) the conditions for confined slip. All of thses conditions can not be preciesely discussed for all examples. The result is justified by a few examples.

In all cases the parameter D seems to play an essential role:

$$D \equiv (\Delta\tau)/K(\delta_c)$$

where often times $K \simeq G/L$.

$\Delta\tau$ is a representative stress change in the friction law, δ_c is a characteristic distance in the friction law, K is the stiffness (stress over slip distance) of a relevant mode of the elastic system, G is an elastic modulus of the bulk material, and L is a characteristic length in the elastic sample.

If the constant D is calculated with the elastic stiffness for the deformation mode of interest then, for linear and (at least approximately) for non-linear analysis, it gives a measure of instability of the given mode. So long as $D<<1$ (or perhaps $D<.5$) slip should be stable to spatial perturbations.

Stability of Steady Sliding

One class of examples in which temporal and spatial instabilities can be compared is for the stability of steady sliding. Consider a sample in which the friction law and the equations for the deformation of the sample admit a steady sliding solution. The sample need not have any special symmetry or have uniform normal stress. In order for uniform sliding to become non-uniform some spatial mode (or modes) must grow in time. It will often be true that the first spatial mode shape to become unstable will correspond roughly to homogeneous slip. This is because, for most

plausible friction laws (Rice and Ruina 1983) stiffness is stabilizing and that for plausable elastic models the least stiff deformation mode corresponds to approximately homogeneous slip.

The argument is made somewhat sharper if one restricts attention to bodies that are reflection-symmetric about the slip plane. In this case slip, even inhomogeneous slip, does not induce any change in normal stress (attributed to discussion with L. Knoppoff in discussion with J. Dieterich).

Slip-Weakening Friction Law

Not all experiments are steady sliding experiments. An example is the case in which slip is initiated from rest. As a special example use a slip displacement friction law. This friction law may be viewed as a rough approximation to a state variable friction law, as motivated in Dieterich (1979), or may just be used as another special case.

Consider this friction law on the boundary between two uniformly stressed homogeneous linear elastic layers (slabs or the ring of contact on a rotary shear sample). The elasticity may be characterized by the function $k(\kappa)$ where

$$\begin{aligned} &\text{if} && \text{slip displacement} = && \sin[\kappa(x-x_o)] \\ &\text{then} && \text{shear stress} && = k(\kappa)\sin[\kappa(x-x_o)]. \end{aligned}$$

For periodic boundary conditions (as with a rotary shear sample) κ can only take on discrete values. For an infinite layer κ can take any

positive real value. κ=0 corresponds to homogeneous slip and it is expected that in general that the stiffness associated with homogeneous slip is less than the stiffness for any other mode of slip: $k(\kappa>0)>k(0)$. If the remote boundary conditions are traction (or load) then $k(0)=0$. For remote displacement conditions $k(0)>0$.

Three simple questions can now be addressed: Are small perturbations from a given homogeneous slip solution unstable for any κ? Are small perturbations from from a given homogeneous slip solution unstable for κ=0? Can the sample support a shear fracture?

To address these questions the friction law is characterized as in figure A1. The peak stress which may occur sometime after stress initiates is τ_{peak}, the residual relaxed stress is τ_r which occurs after slip δ_c, the area under the curve is , and the slope of the curve at a given point is $d\tau/d\delta$. Slip weakening is indicated coursely since $\mathcal{G}>0$ and, in detail, by points on the slip curve having negative slope.

If slip is progressing uniformly due to remotely applied displacements then a given mode of slip is unstable if $k(\kappa)<-d\tau/d\delta$. Since $k(0)<k(\kappa>0)$ the first mode to be unstable is mode 0 (homogeneous slip). So if homogeneous slip is temporally stable then all spatial modes are temporally stable.

But even if small perturbations cannot grow one might consider the possibility of finite perturbations being unstable. One special case of a finite perturbation is shear fracture where there is a large region on the surface which has undgone slip of δ_c or more and a separate region which as undergone little or no slip. The two regions are separated by the endzone (process zone) of the fracture. A finite shear fracture is only possible if 1) the load associated with the remote applied displacement is less than τ_{peak} and 2) if it is energetically favorable. These two conditions are true if there exists a line as shown in figure A1. The slope is -k(0) and its location is determined such that it cuts the τ vs δ curve into two equal area sections as shown. Such a diagram is only possible if the maximum value of $-d\tau/d\delta$ on the friction curve is greater than k(0); the same condition as for temporal instabilities with spatially homogeneous slip. Thus fracture is only possible if homogeneous slip would lead to stick-slip.

State Variable Friction Laws

Non-linear numerical simulations using a rate and state dependent friction law also show that unless homogeneous slip is unstable that spatial instabilities do not grow (Horowitz and Ruina 1986?!).

Conclusion of Appendix 1

A constitutive law that is inferred from measurement can be given a consistency check: If it implies that homogeneous slip is stable than it is consistent with an un-localized slip. This does not prove, however, that localized slip did not occur.

One can imagine an example where the friction law would, because of localised slip and macroscopic measurement, lead to the perception of an averaged and incorrect friction law. This incorrect friction law might not predict localised slip. Consider, for example, a roughly rate independent friction law that has slip weakening and also some kind of healing mechanism. Apply this friction law to a rotary shear sample that is sufficiently large and compliant to contain a shear fracture with this material. Then during constant rate slip, the fracture could propagate around and around the sample at a rate proportional to the remote loading rate. The measured load would be approximately independent of nominal rate. Thus the inferred friction law would be neither rate nor displacement dependent. This friction law would pass the test for not implying localized deformation, even though such deformation was responsible for the observed behavior.

It is not known whether such propagating solutions, if and when they exist, would be stable. In the case of the particular state variable law being used by Horowitz and Ruina (1986) such circular propagating solutions were numerically found to exist but were unstable.

Though we have shown that localised slip *is not* expected when slip is *stable*, it might well be true that localised slip *is* expected when slip is *unstable*. The numerical simulations of Horowitz and Ruina (1986) always show imhomogeneous slip when homogeneous slip is more than slightly temporally unstable. Similarly, the simulations of Mavko (1986) and Tse and Rice (1986) show a depth variation of slip in their stick-slip earthquake simulations. The crude two block stick-slip model of Nussbaum and Ruina (1986) also indicates that stick slip is associated with inhomogeneous slip.

APPENDIX 2: Localization of Shear Deformation to Slip

Earthquakes are often associated with fault zones rather than surfaces of slip. Similarly, friction experiments are often performed with a gouge layer. The properties of the layer as a continuum might be inferred from the overall sample deformation and then used to predict earthquake dynamics. However, it is claimed here (following Ruina 1980) that any experiment on gouge material that supports the possibility of stick slip is a localized deformation experiment. Thus neither 1)an earthquake, nor 2) a stick slip experiment with gouge, nor 3) a gouge experiment that predicts stick slip in a different testing machine, can be described with a law for the deformation of a bulk continua. This is demonstrated for three different material laws: 1)Strictly strain rate dependent, 2)strictly strain dependent and 3)strain rate and state dependent.

The homogeneous in properties layer of thickness h is assumed to be deforming in simple shear. The through the thickness direction is y ($0 \le y \le h$). The deformation is assumed to be homogeneous along surfaces parallel to the plane of the fault. The allowed deformation may be viewed as that of a shearing deck of cards. If other deformation modes were allowed, and the constitutive description was generalized to include them, the conditions for the onset of localization would be less restrictive.

If the constitutive law for the gouge layer is that $\tau = f(\dot{\gamma})$ where $\dot{\gamma}$ is the deformation rate then homogeneous deformation through the thickness is only stable if $df/d\dot{\gamma} > 0$ as discussed by Rabinowicz (1957). However in a spring block model for stability with this constitutive law, instability

always occurs when the incremental viscous damping is negative, that is if $d\tau/d\dot{\delta}<0$ (where $\dot{\delta}\equiv\dot{\gamma}h$). Thus, for $\tau=f(\dot{\gamma})$, instability is only possible with strain rate weakening, but strain rate weakening implies localization of deformation.

If, on the other hand, $\tau=f(\gamma)$ the condition for localization of deformation is that $df/d\gamma<0$. However, elastic instabilities require that $df/d\delta<-k<0$. That is, the conditions for localization are met before the conditions for elastic instability with a homogeneously deforming layer.

Localization of Deformation with a State Variable Friction Law

The constitutive law for deformation of the general type proposed in Dieterich 1979 as expressed in Ruina (1983) might, if expressed in terms of deformation, have the form:

$$\tau = F(\theta(y),\dot{\gamma}(y))$$
$$\dot{\theta}(y) = G(\theta(y),\dot{\gamma}(y)) \quad .$$

τ does not depend on y because of force balance (neglecting inertia). The functions F and G are expected to satisfy certain restrictions in general (Ruina 1983), in particular that $\partial F/\partial\dot{\gamma}>0$ (positive instantaneous viscosity - otherwise localisation follows immediately with no further discussion), $\partial F/\partial\theta>0$ (sign convention on the meaning of state), and that $\partial G/\partial\theta<0$ (Implies stable evolution to steady state at fixed $\dot{\gamma}$). Consider a homogeneous deformation $\tau_h(t)$, $\theta_h(t)$, $\dot{\gamma}_h(t)$ that satisfies the

constitutive law as well as some given boundary conditions which may or may not be imposed by means of an interposed spring. Now consider another set of functions $\tau(t)$, $\theta(y,t)$, $\gamma(y,t)$ which solve the governing equations and the boundary conditions, and which are close to the homogeneous solution so that the governing equations can be linearized about the homogeneous deformation.

Define $\Delta\theta \equiv \theta(y_1,t) - \theta(y_2,t)$ where y_1 and y_2 are two points of interest in the layer such that $\Delta \geq 0$. Define $\Delta\dot{\gamma}$ similarly. $\Delta\tau$ must be zero by force balance (again). For deformation far from steady state the measure of inhomogeneity is somewhat arbitrary. For purposes of calculation convenience we use the inhomegneity of the state $\Delta\theta$ as a measure of the localisation of deformation. In particular we associate $\Delta\dot{\theta} > 0$ with localisation.

Linearization of the constitutive law gives:

$$0 = \Delta\tau = F_\theta \Delta\theta + F_{\dot{\gamma}} \Delta\dot{\gamma}$$
$$\Delta\dot{\theta} = G_\theta \Delta\theta + G_{\dot{\gamma}} \Delta\dot{\gamma}$$

where the subscripts indicate partial derivatives to be evaluated at the values of θ_h and $\dot{\gamma}_h$ in the corresponding homogeneous deformation. These equations can be re-expressed as:

$$\Delta\dot{\theta} = [G_\theta / F_{\dot{\gamma}}] (d\tau / d\dot{\gamma}) \Big|_{\dot{\theta} \text{ fixed}} \Delta\theta$$
$$\Delta\dot{\gamma} = -(F_\theta / F_{\dot{\gamma}}) \Delta\theta$$

Since $[G_\theta/F^\bullet_\gamma]$ is greater than 0 by assumption the condition for localization $\Delta\dot{\theta}>0$ is that $(d\tau/d\dot{\gamma})\big|_{\dot{\theta}\ \text{fixed}}>0$. Though further interpretation is shown in Ruina (1980) we can most simply interpret this result at steady sliding where the condition reduces to $d\tau/d\dot{\gamma}_{\text{steady state}}<0$. This result can also be derived by looking at the special subset of spatial perturbations for which $\tau=\tau_h$ in which case the instability of steady sliding with constant force loading implies localisation directly (whether or not the boundary condition is "dead" loading). The condition $d\tau/d\dot{\gamma}_{\text{steady state}}<0$ for localisation is less severe than the condition for unsteady slip for machines with all but zero stiffness. Thus again we find that the possibility of temporal instabilities depends on the deformation having localised to a surface (or, at least to a size scale that is smaller than that of the validity of the continuum description). It is also possible that that: a continuum approximation is not appropriate at any size scale, or even if valid in certain regions that other modes of localisation have broken up the smoothness of the deformation field.

The conclusions of this appendix are consistent with the work of Chester and Logan (1985) where they associated gouge structure (localisation bands) with rate weakening and stick slip. Also, the gouge experiments of Dieterich (1981) showed no scaling of the characteristic slip distance with gouge layer thickness thus indicating inhomogeneous deformation.

APPENDIX III: A Rate Scaling Rule

The rate scaling rule derived in Ruina (1980) and mentioned in Ruina (1983) applies to any constitutive relation of the form:

$$\tau = \tau_o + \sum[B_i \ln\theta_i] + A\ln(\dot{\delta})$$
$$d\theta_i/dt = G_i(\theta_i, \dot{\delta}) \quad \text{for all } i.$$

This form includes both the simple one and two state variable law proposed in Ruina 1983 and used in Gu et al (1984), Tullis and Weeks (1985), Mavko (1981, 1983, 1986), Tse and Rice (1986) and also works with other rules for the evolution of state of the type that do evolve during true stationary contact (see Ruina 1983 for a list of candidate evolution laws).

The rate scaling rule, assumes that 1) inertia is neglected, 2) elasticity is linear, and 3) that normal stress is constant. It states that: If a given load point history (expressed as slip rate vs time $\dot{u}(t)$) is run at fast or slow motion ($s\dot{u}(st)$) with scaling rate s, then the same friction stress vs slip curve results in both cases (offset by a constant).

In the case of 'static' friction tests described in the text, two tests that have the same value of $v_o t_o$ are two tests that are related to each other by a simple scaling. Thus the friction traces look the same for the two cases (offset by a constant) and the apparent jump in μ is the same for the two tests.

ACKNOWLEDGEMENTS: Kianoosh Nagshineh, John Recker and Jenny Michaels for programming assistance; Jason Cortell, Jan Cornelius, Dan Azari, Dan Burnside and Jeff Schwardt for electrical and mechanical design and construction; Instron Co. personell for technical advice; Jim Dieterich for the use of his laboratory and many helpful ideas and suggestions; Jim Rice for encouragement and technical advice; Jim Papadopoulos for 567 technical and editorial suggestions; Richard Garwin for suggesting an air bearing; Charles Stone of the Arkansas Geological Commission for providing the Navaculite specimens; William Olson for discusion of his experiments; Terry Tullis and Renata Dmowska for encouragement; John Weeks for editorial comments; and the US Geological Survey Earthquake Hazards Reduction Program and The National Science Foundation for funding.

REFERENCES

Barton, Nick, 'Some size dependent properties of joints and faults', Geophysical Research Letters, Vol. 8, No. 7, 667-670, 1981

Brace, W.F. and Byerlee, J.D., 'Stick-slip as a mechanism for earthquakes', Science, 153, 990-992, 1966

Byerlee, J.D., 'The mechanics of stick-slip', Tectonophysics, 9, 475-486, 1970

Byerlee, J., 'Friction of Rocks', Pure Appl. Geoph., vol. 116, 615-626, 1978

Chester, *.*., and Logan, J., 'Correlation of Gouge Texture and Velocity Dependence', EOS, vol 66, 1100-1101, 1985

Dieterich, J.H., 'Time-dependent friction in rocks', J. Geophys. Res., Vol. 77, 3690-3697, 1972

Dieterich, J.H., 'Time-dependent friction and the mechanics of stick slip, Pure Appl. Geophys., Vol 116, 790-806, 1978

Dieterich, J.H., ' Modeling of rock friction, 1, Experimental results and constitutive equations', J. Geophys. Res., Vol. 84, 2161-2168, 1979a

Dieterich, J.H., ' Modeling of rock friction, 2, Simulation of preseismic slip', J. Geophys. Res., Vol. 84, 2169-2175, 1979b

Dieterich, J.H., 'Experimental and model study of fault constitutive properties', in Solid Earth Geophysics and Geotechnology, edited by S. Nemet-Nasser, 21-30, American Society of Mechanical Engineers, New York, 1980

Dieterich, J.H., 'Constitutive properties of faults with simulated gouge', in Mechanical Behavior of Crustal Rocks, Geophys. Monogr. 24, edited by N.L. Carter, M. Friedman, J.M. Logan and D.W. Stearns, 103-120, AGU, Washington, D.C., 1981

Dieterich, J.H. and G. Conrad, 'Effect of humidity on time-and velocity-dependent friction in rocks', J. Geophys. Res., Vol. 89, 4196-4202, 1984.

Gu, Ji-Chang, J.R. Rice, A. Ruina and S.T. Tse, 'Slip motion and stability of a single degree of freedom elastic system with rate and state dependent friction, J. Mech. Phys. Sol., 32,167-196,1984.

Hobbs, B.E., 'Normal Stress Changes and the Constitutive Law for Rock Friction', EOS, vol 66, #66, pg 382, 1985

Horowitz, F. and A. Ruina, 'Frictional Slip Patterns Generated in a Spatially Homogeneous Elastic Fault Model', submitted to J. Geoph. Res., 1986

Johannes, V.I., M.A. Green, C.A. Brockely, 'The role of the rate of application of the tangential force in determining the static friction coefficient', Wear, Vol 24, 381-385, 1973

Johnson, T., 'Time dependent friction of granite: Implications for precursory slip on faults', J. Geophys. Res., Vol. 86, 6017-6028, 1981

Kosloff, D.D., and H.-P. Liu, 'Reformulation and discussion of mechanical behavior of the velocity-dependent friction law proposed by Dieterich', Geophys. Res. Lett., Vol. 7, 913-916, 1980

Lockner, D.A., and J.D. Byerlee, 'Laboratory Measurements of Velocity-Dependent Frictional Strength', Open-File Report 86-417, US Geological Survey, 345 Middlefield Rd., Menlo Park, CA 94025, 1986.
Mavko, G.M., 'Simulation of creep events and earthquakes on a spatially variable model', Eos Trans. AGU, 61, 1120, 1980

Mavko, Gary, 'Simulation of Large-Scale Earthquake Cycles by Using a Laboratory Friction Law', Eos Trans. AGU, 64, 851, 1983

Mavko, G.M., 'Large-scale earthquakes from a laboratory friction law', J. Geophys. Res., in press, 1986.

Okubo, P.G., and J.H. Dieterich, 'Effects of Physical Fault Properties on Frictional Instabilities Produced on Simulated Faults', J. Geophys. Res., Vol 89, B7, 5817-5827, 1984

Okubo, P.G., and Dieterich, J.H., 'State Variable Fault Constitutive Relations for Dynamic Slip', in EARTHQUAKE SOURCE MECHANICS, Geophys. Monograph 37, Maurice Ewing Volume 6, Ed. S. Das, J. Boatwright, and C.H. Scholz, pp25-35, Am. Geophys. Union, Washington, DC, 1986

Olsson, W.A., 'A Constitutive Model for Frictional Slip on Rock Interfaces', Mechanics of Materials, vol 3, 295-299, 1984

Olsson, W.A., 'Normal Stress History Effects on Friction Stress in Tuff', vol. 66, #46, 1101, 1985

Olsson, W.A., 'Rock Joint Compliance Studies', SANDIA report #86-0177, Albuquerque, NM 87185, 1986.

Olsson, W.A., 'The Effects of Changes in Normal Stress on Rock Friction', submitted to 2nd Int'l Conf. on Constitutive Laws for Eng. Mat's, Tucson, 1987

Palmer, A.C. and J.R. Rice, 'The growth of slip surfaces in the progressive failure of over-consolidated clay', Proc. Roy. Soc. Lond. A., Vol. 332, 527-548, 1973

Rabinowicz, E., 'The intrinsic variables affecting the stick slip process', Proc. Phys. Soc. London, Vol 71, 668-675, 1958

Rice, J.R., 'Constitutive Relations for Fault Slip and Earthquake Instabilities', Pure and Applied Geophysics, vol 121, 443-475, 1983

Rice J.R. and J.-C. Gu, 'Earthquake Aftereffects and Triggerred Seismic Phenomena', Pure and Applied Geophysics, 121, 187-219, 1983

Rice, J.R. and A. Ruina, 'Stability of steady frictional sliding', J. Appl. Mech., Vol 50, 343-349, 1983

Rice, J.R. and S.T. Tse, 'Dynamic motion of a single degree of freedom elastic system with rate and state dependent friction', J. Geophys. Res., Vol. 91, 521-530, 1986.

Ruina, A.L., 'Friction Laws and Instabilities: A quasistatic analysis of some dry frictional behavior', PhD Thesis, Brown Univ. Providence, RI, 1980

Ruina, A.L., 'Slip instability and state variable friction laws', J. Geoph. Res., Vol. 88, 10359-10370, 1983.

Ruina, A.L., 'Constitutive relations for frictional slip', in Mechanics of Geomaterials, Z. Bazant, ed., John Wiley & Sons Ltd., London, 1985.

Sakamoto, T., J. Tanii, and T. Tsukizoe, 'A Friction Apparatus for Measuring the Normal Displacement of a Sliding Body', J. Phys. E., Vol. 13, 1017-1020, 1980

Shimamoto, T., 'Transition Between Frictional Slip and Ductile Flow for Halite Shear Zones at Room Temperature', Science, Vol. 231, 711-714, 1986

Stesky, R.M., 'The Mechanical Behavior of Faulted Rock at High Temperature and Pressure', PhD thesis, MIT, Cambridge, MA, 1975

Teufel, L.W., 'Frictional instabilities in rock: Effect of stiffness, normal stress, sliding velocity and rock type', paper presented at the 18th Annual Meeting, Soc. for Eng. Sci., Brown Univ., Providence, RI, 1981 (also in review for Geoph. Res. Lett.)

Tse, S.T., and Rice, J.R., 'Crustal Earthquake Instability in Relation to the Depth Variation of Frictional Slip Properties', Journal of Geophysical Research, Vol. 91, No. B9, 9452-9472, 1986

Weeks, J., and Tullis, T., 'Frictional Sliding of Dolomite: A Variation in Constitutive Behavior', J. Geophys. Res., Vol 90, B9, pp7821-7826, 1985

Weldon, R.J., and Sieh, K.E., 'Holocene Rate of Slip and Tentative Recurrence Interval for Large Earthquakes on the San Andreas Fault, Cajon Pass, Southern California', Geol. Soc. of America Bulletin, V. 96, pg 793-812, 1985 Tolstoi, D.M., 'Significance of the normal degree of freedom and natural normal vibrations in contact friction', Wear, Vol. 10, 199-213, 1967

Vaughan, P., and J. Byerlee, 'Frictional Sliding in Saturated Westerly Granite: Effect of Slip Rate', in EARTHQUAKE SOURCE MECHANICS, Geophys. Monograph 37, presented Maurice Ewing Volume 6, Ed. S. Das, J. Boatwright, and C.H. Scholz, pp **-**, Am. Geophys. Union, Washington, DC, 1986

FIGURE CAPTIONS

Figure 1: An idealized sample of a continuum point in a friction experiment. σ is the normal stress, τ the shear stress, δ the slip displacement, and δ_n the surface dilation.

Figure 2a: Cutaway view of rotary shear sample. A raised annulus on the upper sample slips on the flat lower sample.

Figure 2b: Local transducers on rotary shear sample. Fixtures are clamped to the upper and lower samples near the slip surfaces. Each of the fixtures is attached to, but insulated from, one plate of the capacitor used to measure normal displacement. The lower fixture also holds the cantilever displacement transducer which is bent by a pin attached to the upper fixture when the samples rotate relative to each other.

Figure 2c: Sample attachment fixtures. The upper sample is clamped to a fixture which is in turn clamped to a series of load cells and to the upper cross bar of the load frame. The lower sample clamp is attached to a collet on an inner bucket and spherical air bearing. The outer spherical surface of this bearing is part of a rigid outer bucket which is connected by thin straps to the inner fixture. The outer bucket is clamped to the actuator shaft which is hydraulically driven to move vertically and to rotate.

Figure 2d: The load frame for rotary shear tests. The bucket which holds the lower sample is powered by the axial and rotary actuators shown. Course measurement of normal and slip displacement is made with the LVDT and RVDT shown. The space frame is added for torsional rigidity.

Figure 3: Sandwich shear specimen geometry. The sandwich shear experiments were performed in the machine of Dieterich (1979). The copper shims close to the slip surface reduce the induced normal stress changes when friction stress changes. The normal load (horizontal arrows) is held constant by a gas accumulator. The friction load (vertical arrow) was controlled using servocontrol. The height of the side samples $l \simeq 4$ inches, the width $w \simeq 1$ inch.

Figure 4: Schematic of Servocontrol system. Actuator motion causes a distortion of the machine sample system by an amount δ_t of which δ_s is measured by the displacement transducer. Of this displacement only δ is inelastic deformation of the sample. The elastic deformation of the material between the transducer mounts is characterized by the spring constant K_s which is in series with the machine stiffness K_m. The load is carried by both springs and the load cell.

The error signal is composed of the difference between a reference signal from the computer and a feedback signal representing sample displacement. The error signal is fed to a non-linear amplifier whos output is a monotonic function of, and the same sign as, the error signal. The output of this amplifier powers a flow control valve. The actuator moves in response to oil flow from the actuator valve.

Electronic noise from various sources is represented by the single source marked "noise". The feedback displacement signal is composed of a mixture of the transducer signal and the load signal. Depending on the sign of the added signal the stiffness is artificially increased or decreased.

Figure 5a: Step change in slip rate in sandwich shear apparatus. The fluctuation in ~~normal~~ friction stress is of central interest.

Figure 5b: Same as above in rotary shear apparatus.

Figure 6: Results of step change in slip rate over 6 orders of magnitude.

Figure 7: Examples of transients at step changes in slip rate showing ~~positive rate dependence,~~ negative rate dependence, ~~etc.~~ for virgin sample

Figure 8: Long Distance transients at step changes in slip rate.

Figure 9: Effect of machine stiffness on the transient in a nominally static friction experiment.

Figure 10: Shear stress at constant slip rate with step changes in normal stress.

Figure 11: Surface Dilation or compaction after control instabilities is associated with softening or hardening post instability behavior.

Figure 12: Nominal time dependence of static friction.

Figure 13: Thermal pulses from mechanical work and from electrical heating.

Figure 14: The slip δ and friction stress τ during a stick slip event on the sandwich shear apparatus. The slip is seen to be more complicated than that predicted by a one-degree-of-freedom dynamic model.

Figure A1: Slip Weakening Friction Law

Figure A2: Effect of stiffness on the possibility of fracture propagation.

Marked for correction

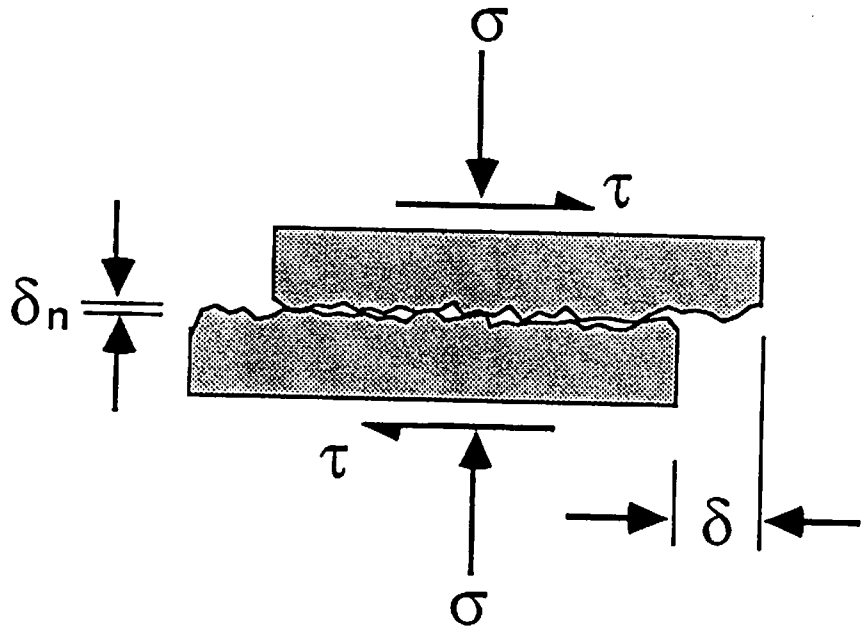

Fig. 1

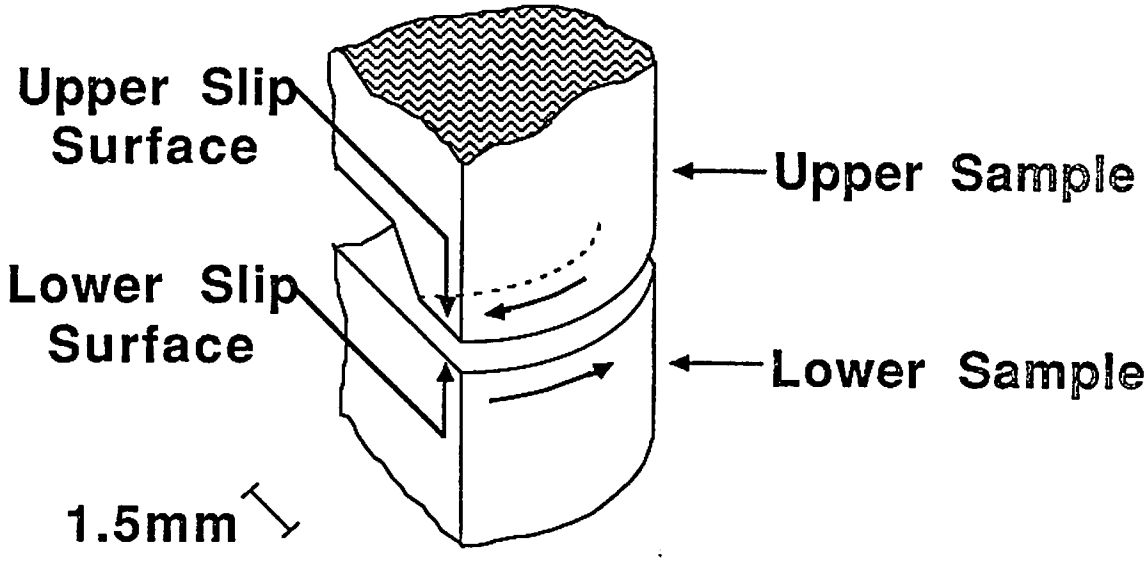
Upper Slip Surface
Lower Slip Surface
1.5mm
Upper Sample
Lower Sample

(a)

Fig. 2a

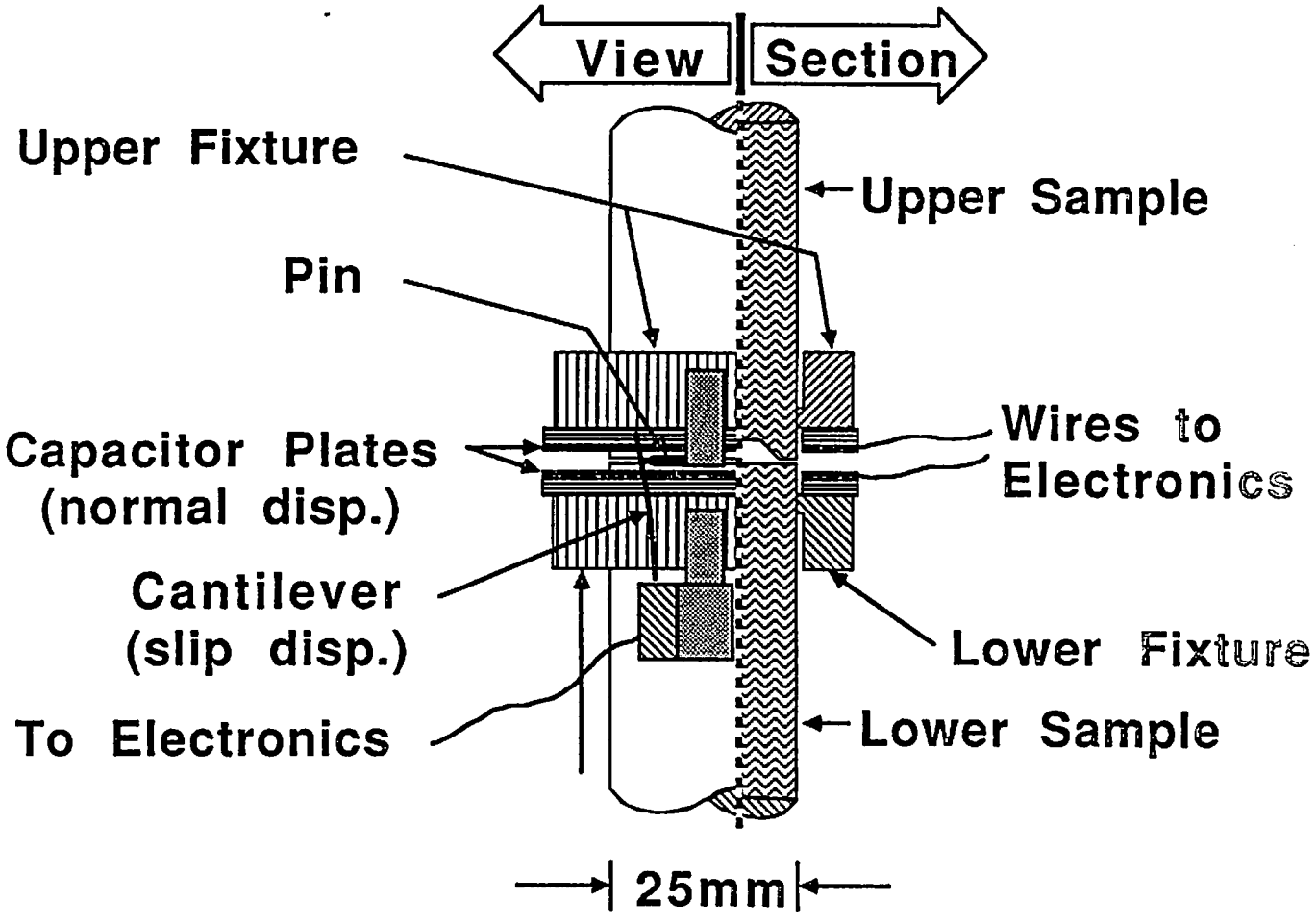
View
Section
Upper Fixture
Upper Sample
Pin
Capacitor Plates
(normal disp.)
Wires to
Electronics
Cantilever
(slip disp.)
Lower Fixture
To Electronics
Lower Sample
25mm

(b)

Fig. 26

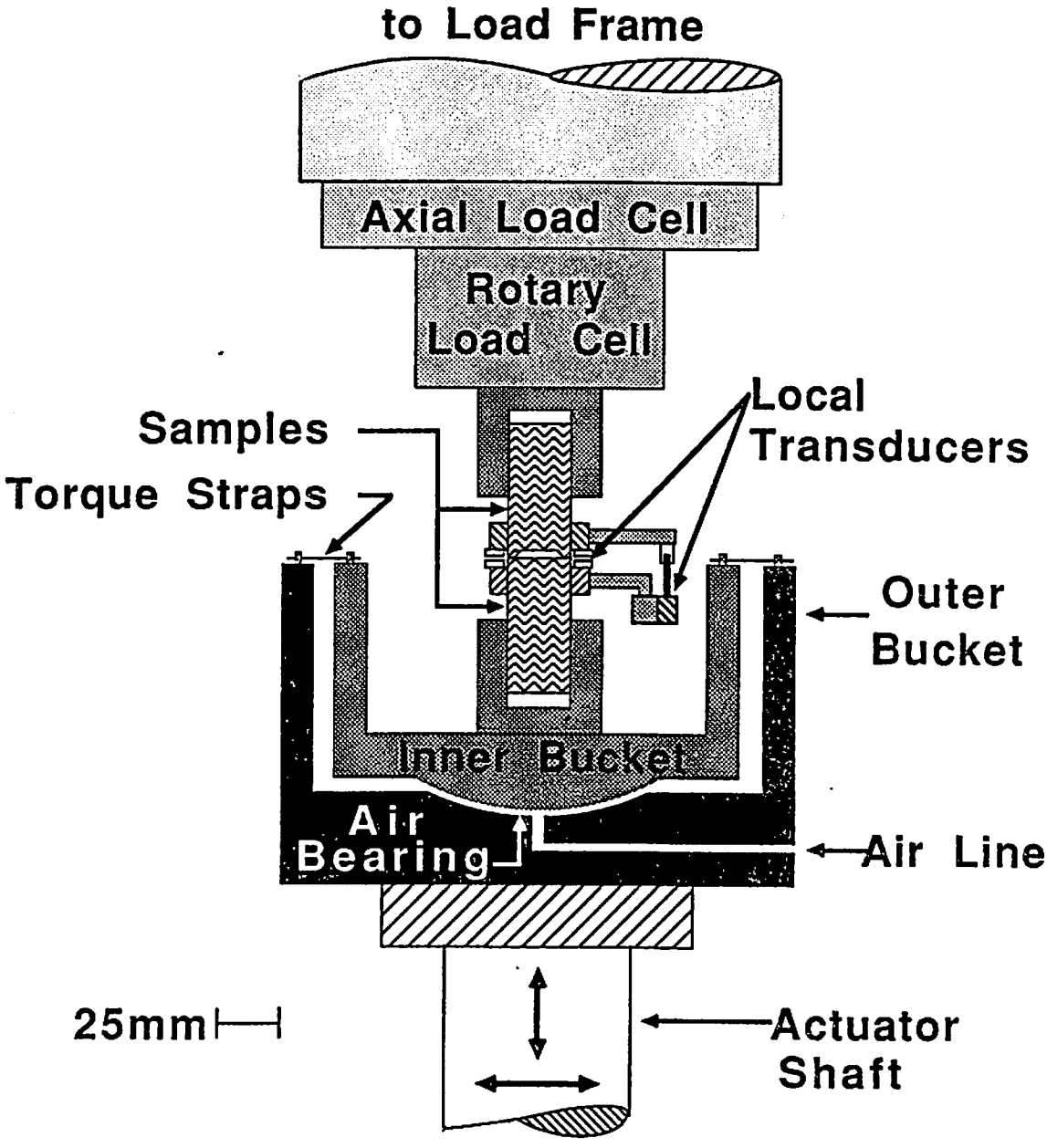
to Load Frame
Axial Load Cell
Rotary Load Cell
Samples
Torque Straps
Local Transducers
Outer Bucket
Inner Bucket
Air Bearing
Air Line
25mm
Actuator Shaft
to Rotary and Axial Actuators, RVDT and LVDT

(c)

Fig. 2c

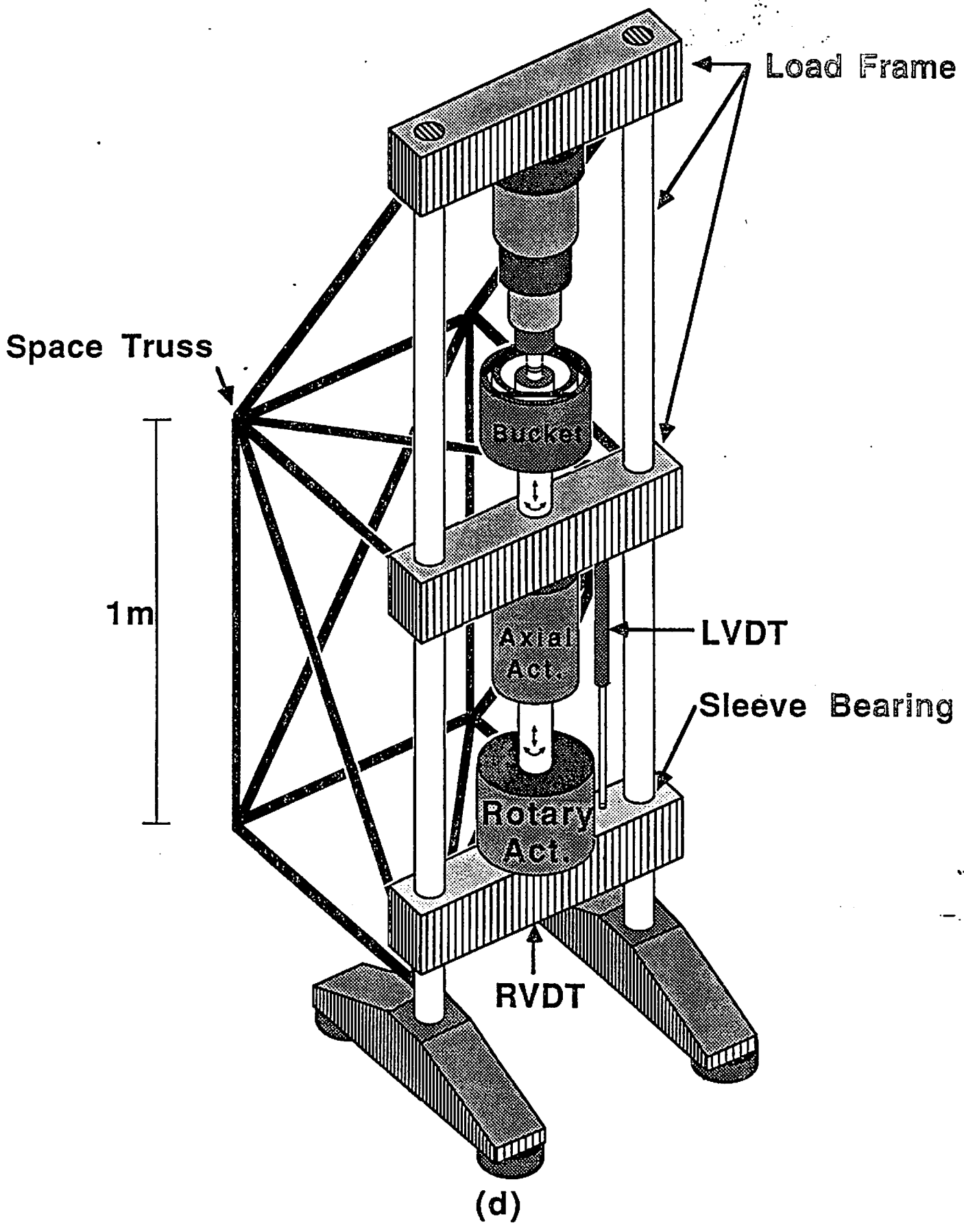
Load Frame
Space Truss
Bucket
1m
Axial Act.
LVDT
Sleeve Bearing
Rotary Act.
RVDT
(d)

Fig. 2d

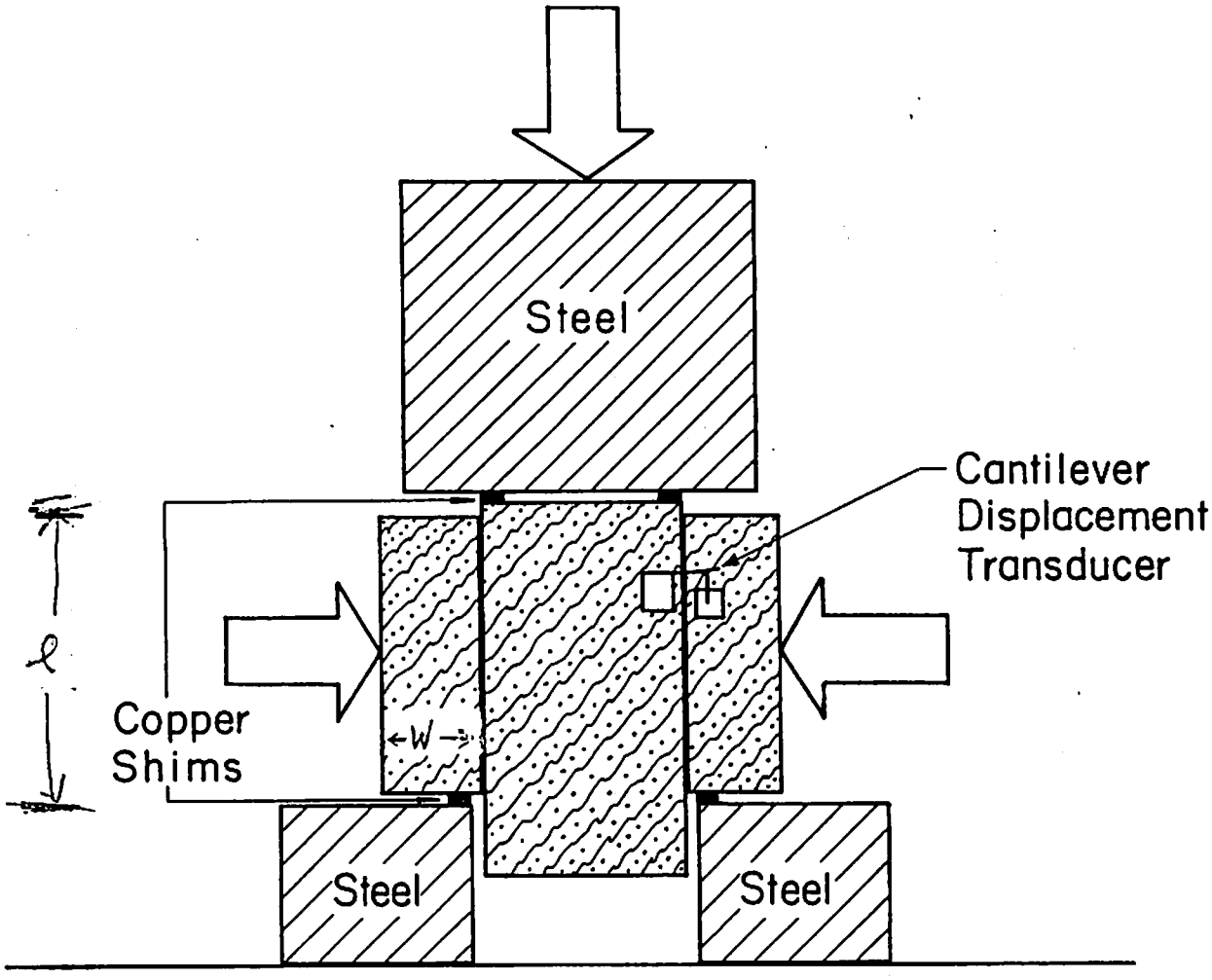
Steel
Cantilever
Displacement
Transducer
ℓ
Copper
Shims
←W→
Steel
Steel

Fig. 3.

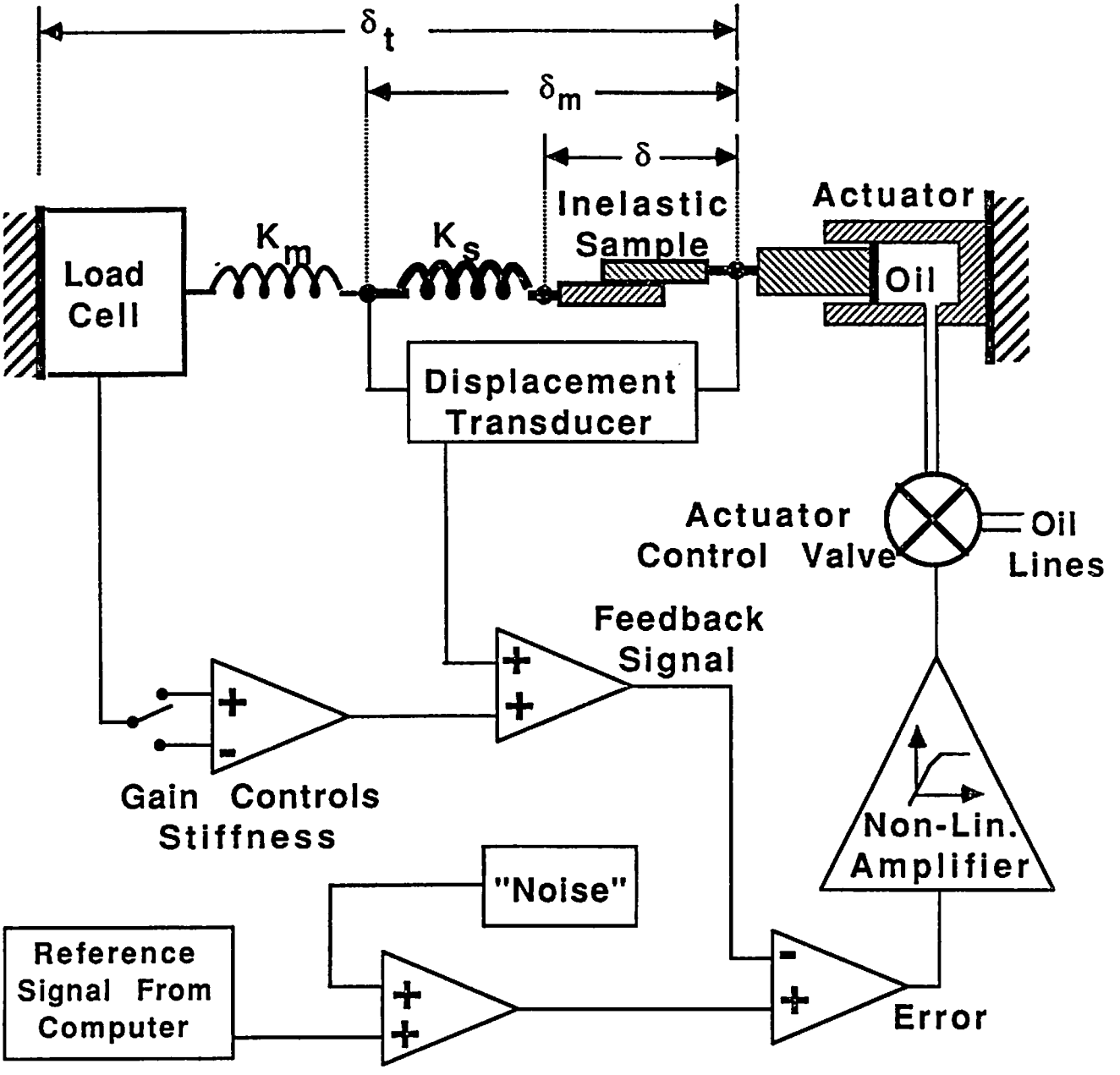
δ_t
δ_m
δ
Inelastic Sample
Actuator
Load Cell
K_m
K_s
Oil
Displacement Transducer
Actuator Control Valve
Oil Lines
Feedback Signal
Gain Controls Stiffness
Non-Lin. Amplifier
"Noise"
Reference Signal From Computer
Error

Fig. 4

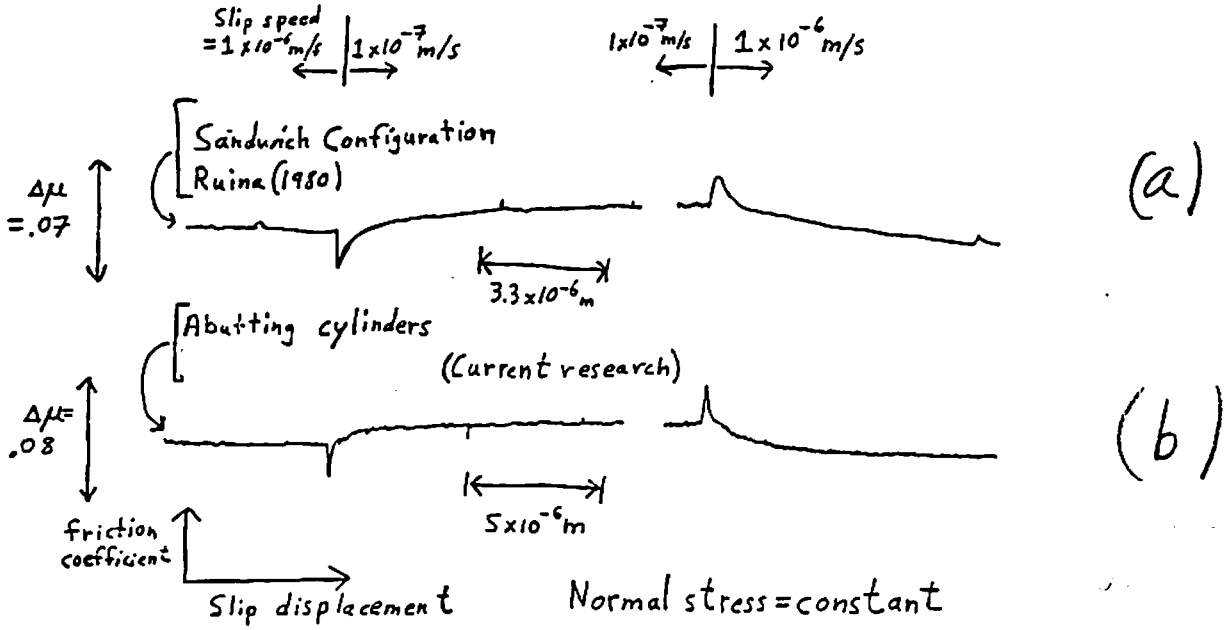
Slip speed
$=1\times10^{-6}$ m/s
1×10^{-7} m/s
1×10^{-7} m/s
1×10^{-6} m/s
Sandwich Configuration
Ruina (1980)
$\Delta\mu$
$=.07$
(a)
3.3×10^{-6} m
Abutting cylinders
(Current research)
$\Delta\mu=$
$.08$
(b)
5×10^{-6} m
friction coefficient
Slip displacement
Normal stress = constant

Figure 5

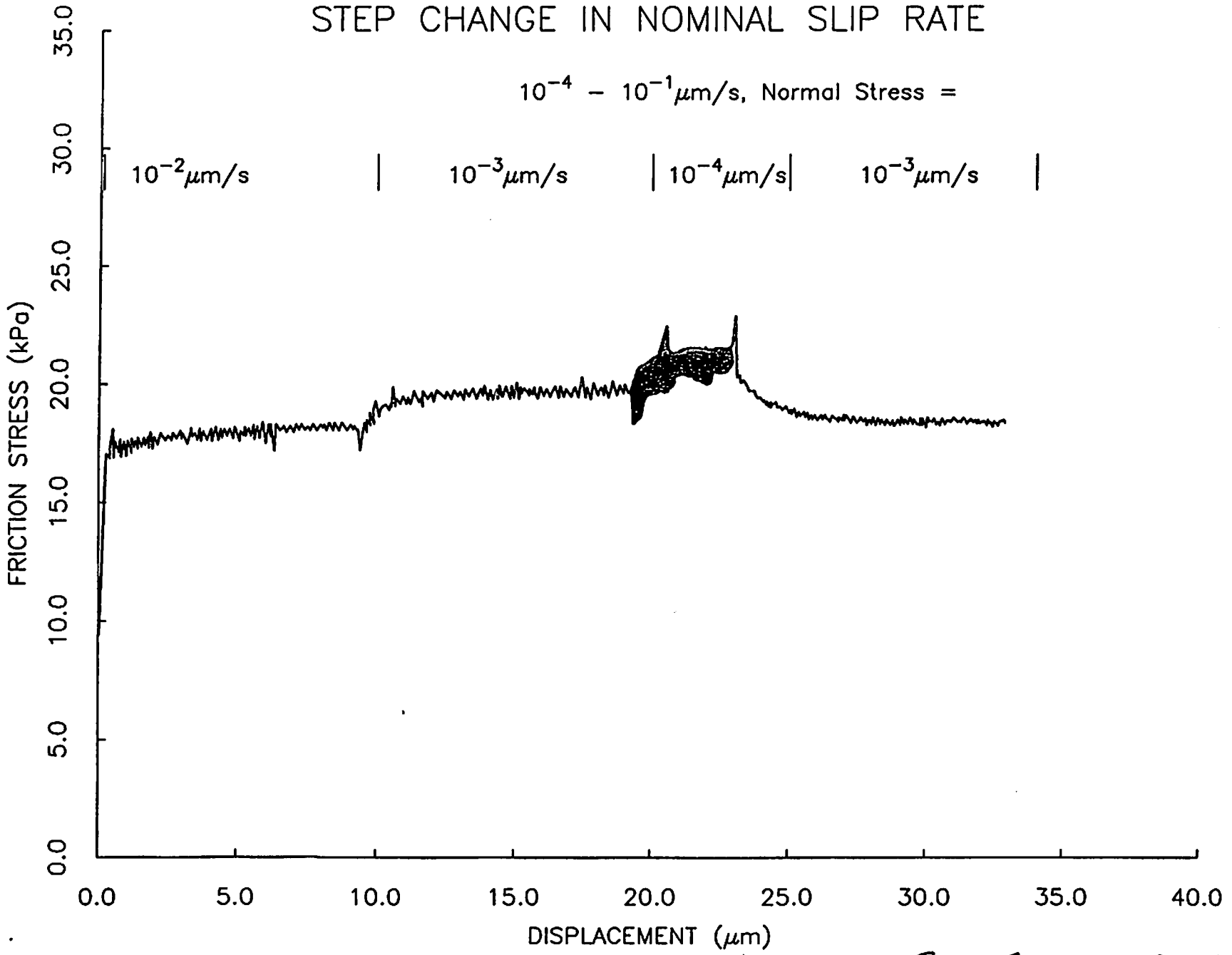

Fig 6 cont'd from last fig

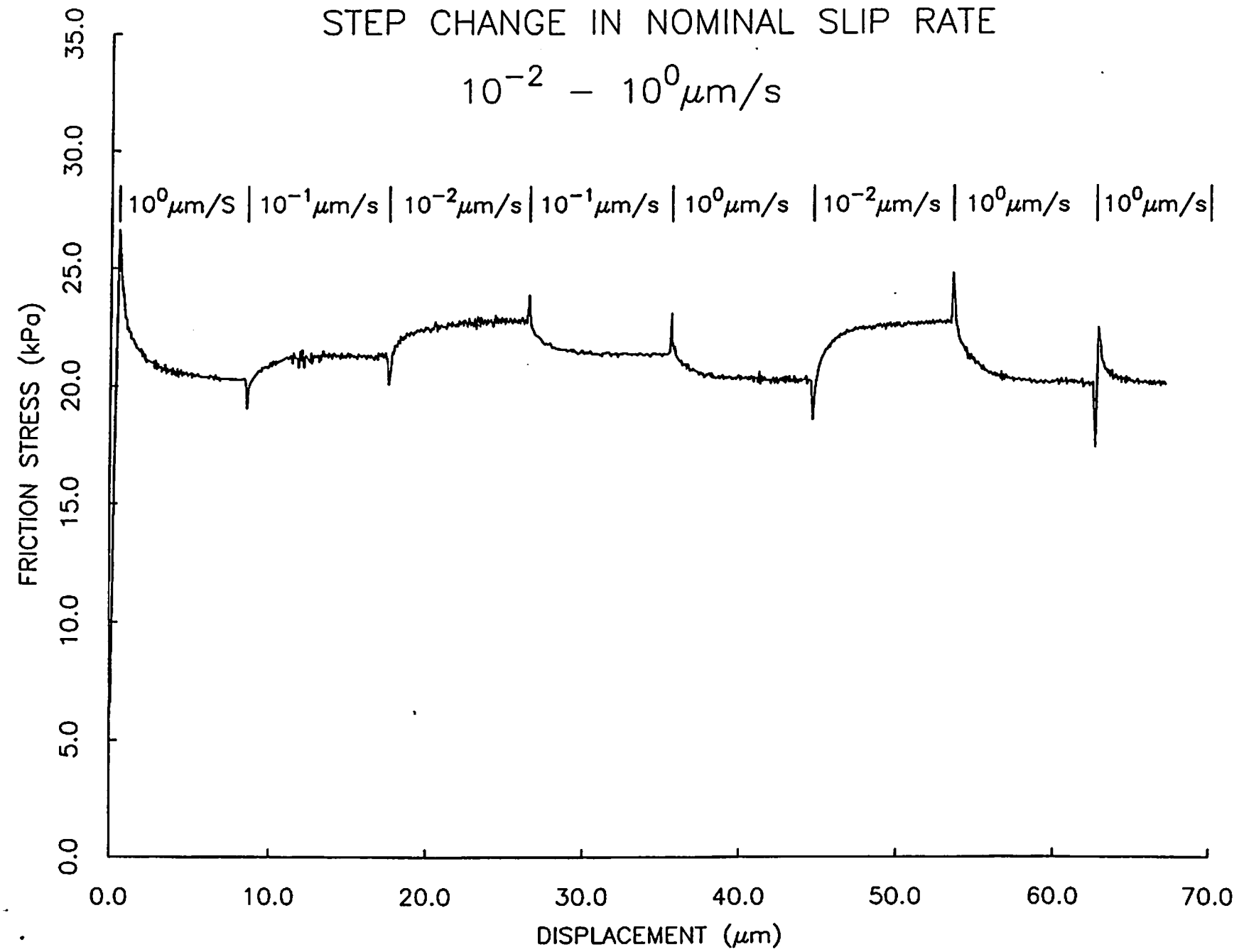

Fig. 6. (cont'd next fig.)

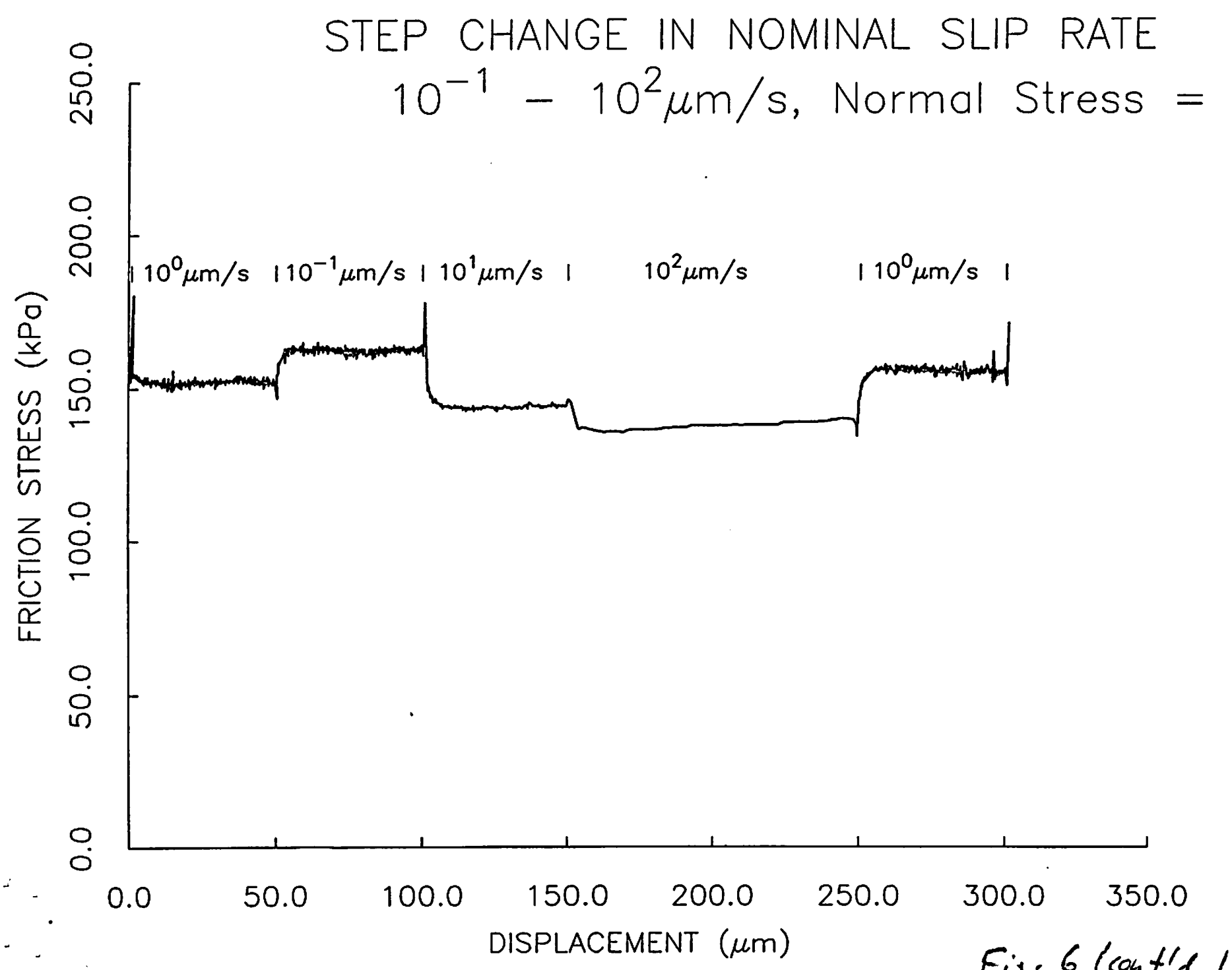
STEP CHANGE IN NOMINAL SLIP RATE
10^{-1} – $10^{2}\mu$m/s, Normal Stress =
$10^{0}\mu$m/s
$10^{-1}\mu$m/s
$10^{1}\mu$m/s
$10^{2}\mu$m/s
$10^{0}\mu$m/s
FRICTION STRESS (kPa)
0.0
50.0
100.0
150.0
200.0
250.0
0.0
50.0
100.0
150.0
200.0
250.0
300.0
350.0
DISPLACEMENT (μm)

Fig. 6 (cont'd)

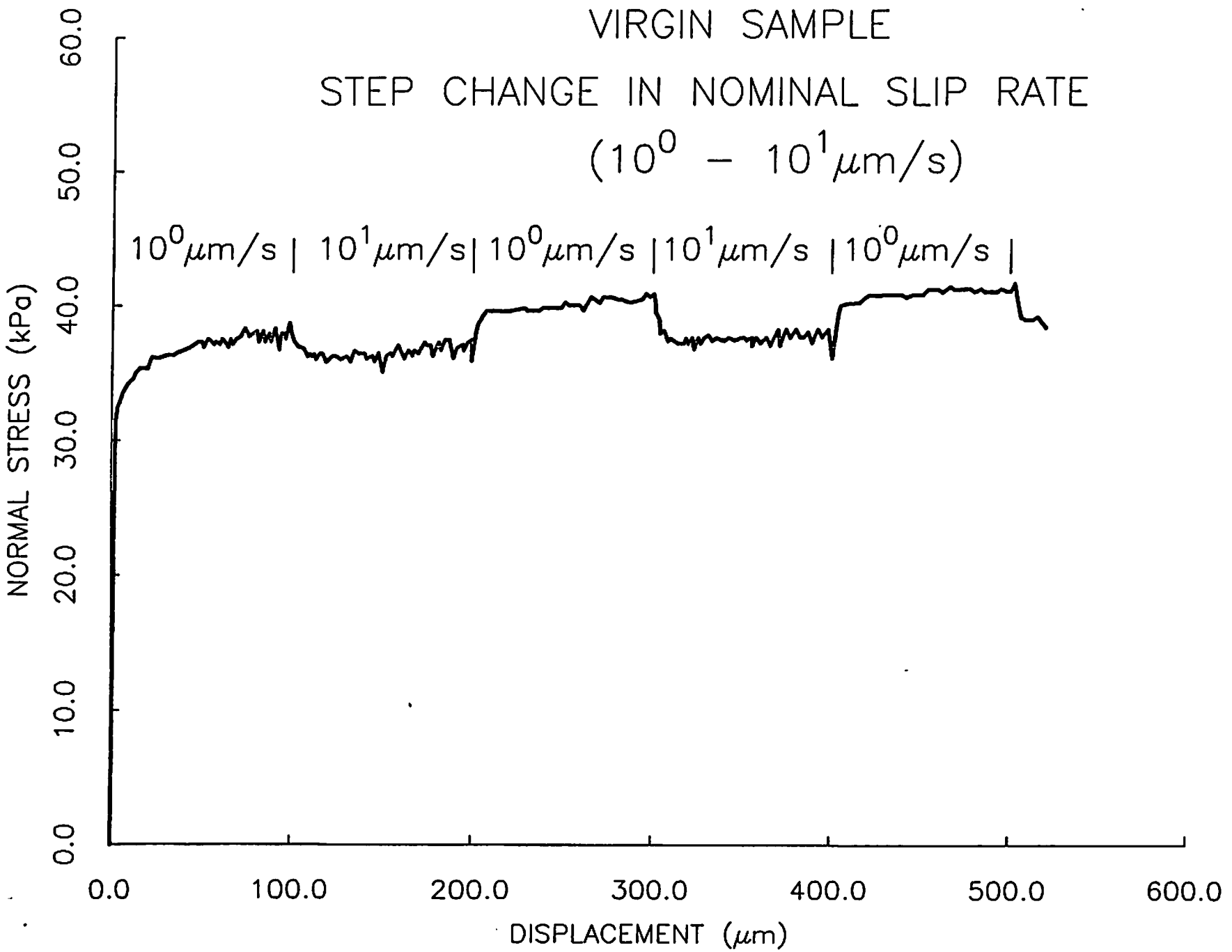
VIRGIN SAMPLE
STEP CHANGE IN NOMINAL SLIP RATE
(10^0 – 10^1 μm/s)
10^0 μm/s | 10^1 μm/s | 10^0 μm/s | 10^1 μm/s | 10^0 μm/s |
NORMAL STRESS (kPa)
0.0
10.0
20.0
30.0
40.0
50.0
60.0
0.0
100.0
200.0
300.0
400.0
500.0
600.0
DISPLACEMENT (μm)

Fig. 7

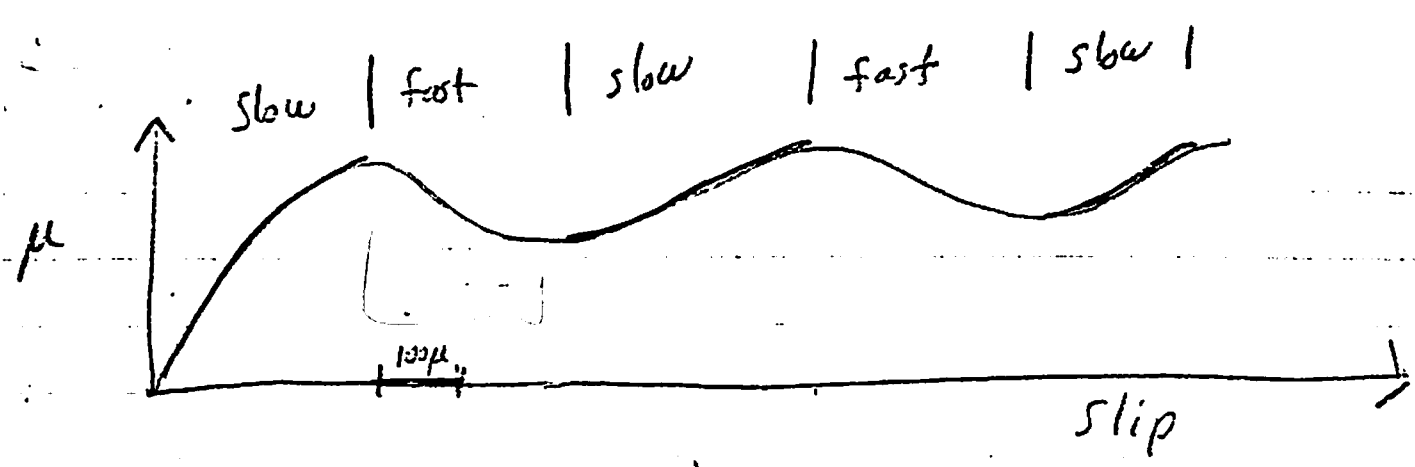

(a)

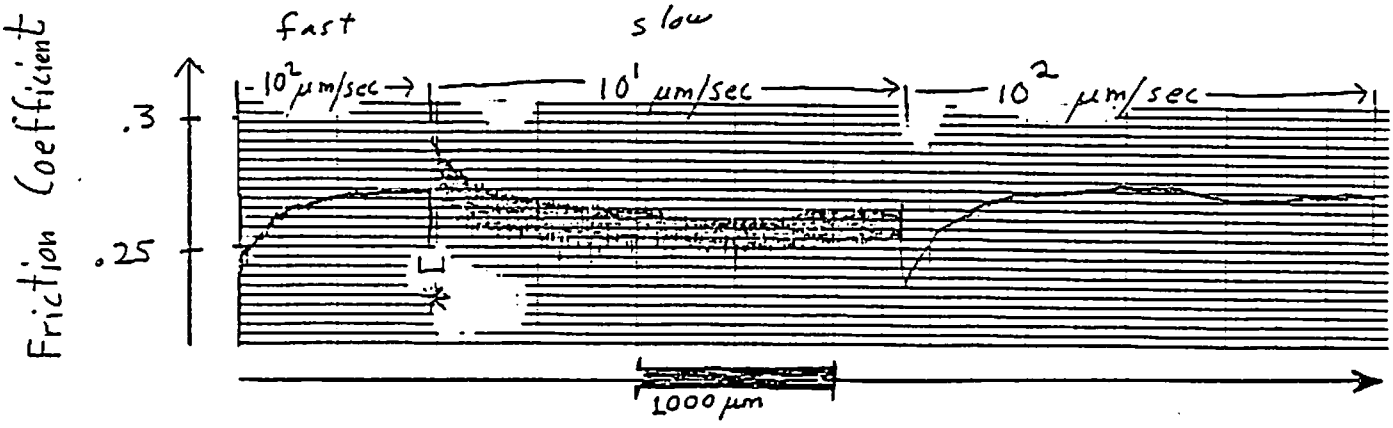

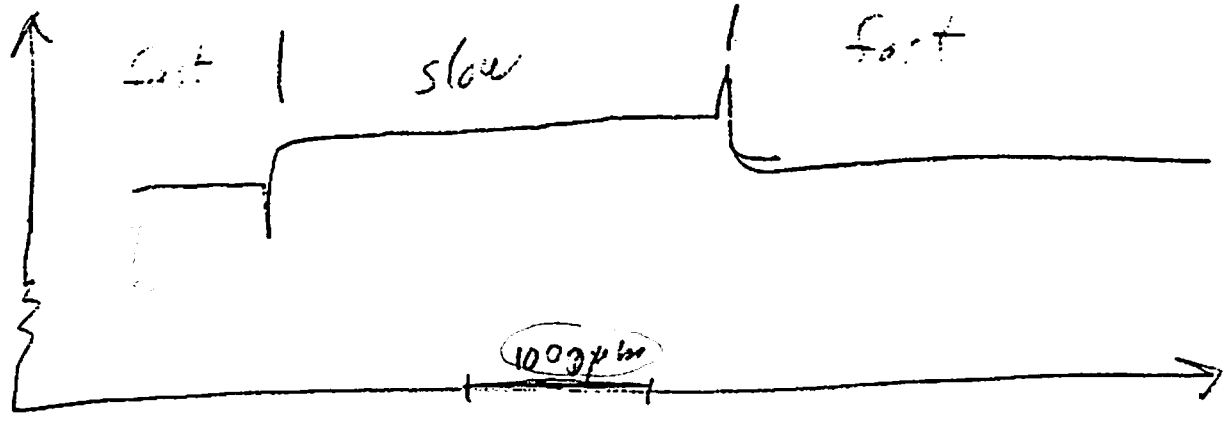

FIGURE 8, Long Distance Transients

(a) Sandwich
(b) Rotary Shear
→ (c) Rotary Shear, No Long Dist Transients

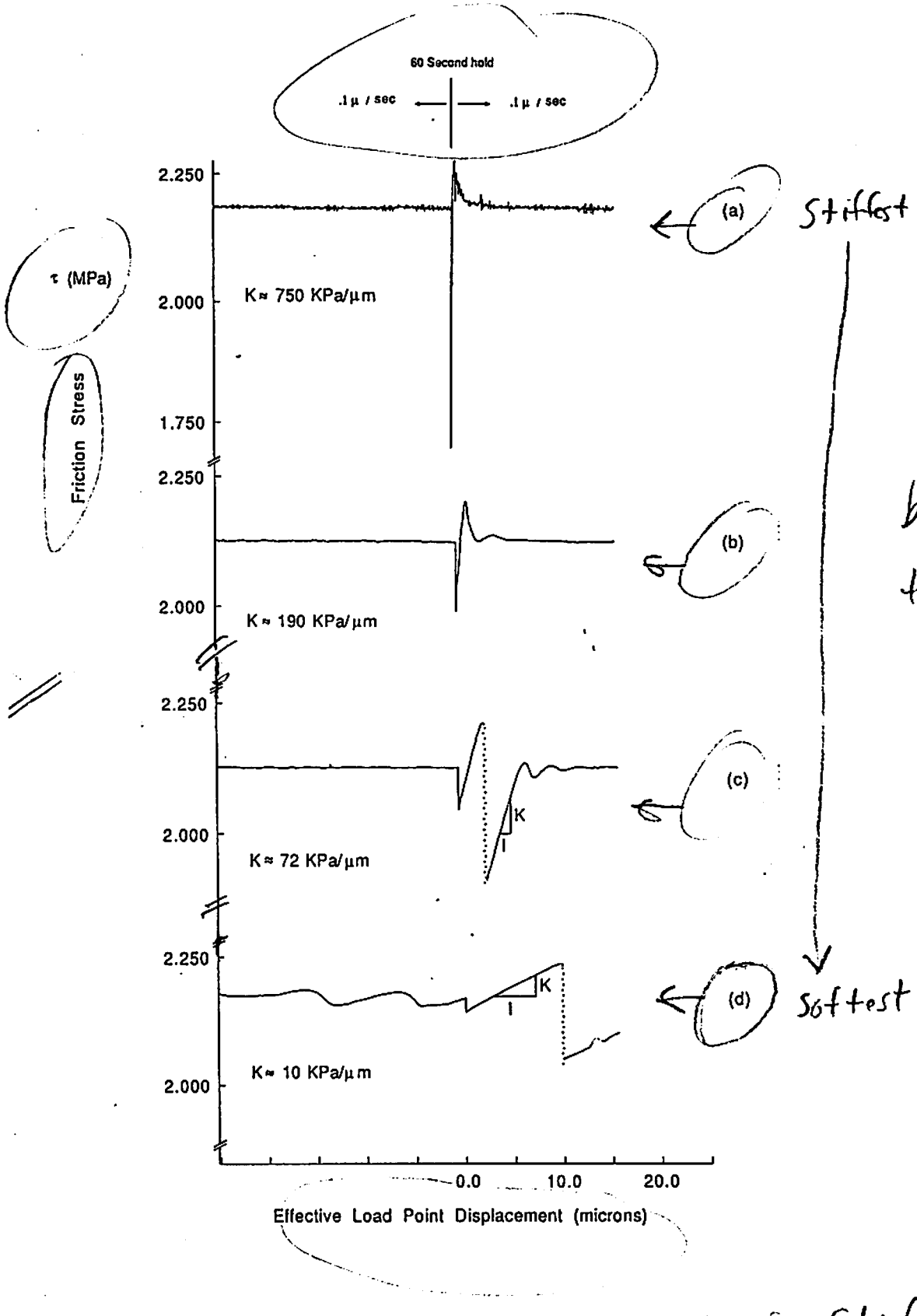

bigger better thanfast

FIGURE 9. Effects of Stiffness.

FIGURE 10(A): STEP CHANGE IN NORMAL STRESS
NOMINAL SLIP RATE = .2 μm/s

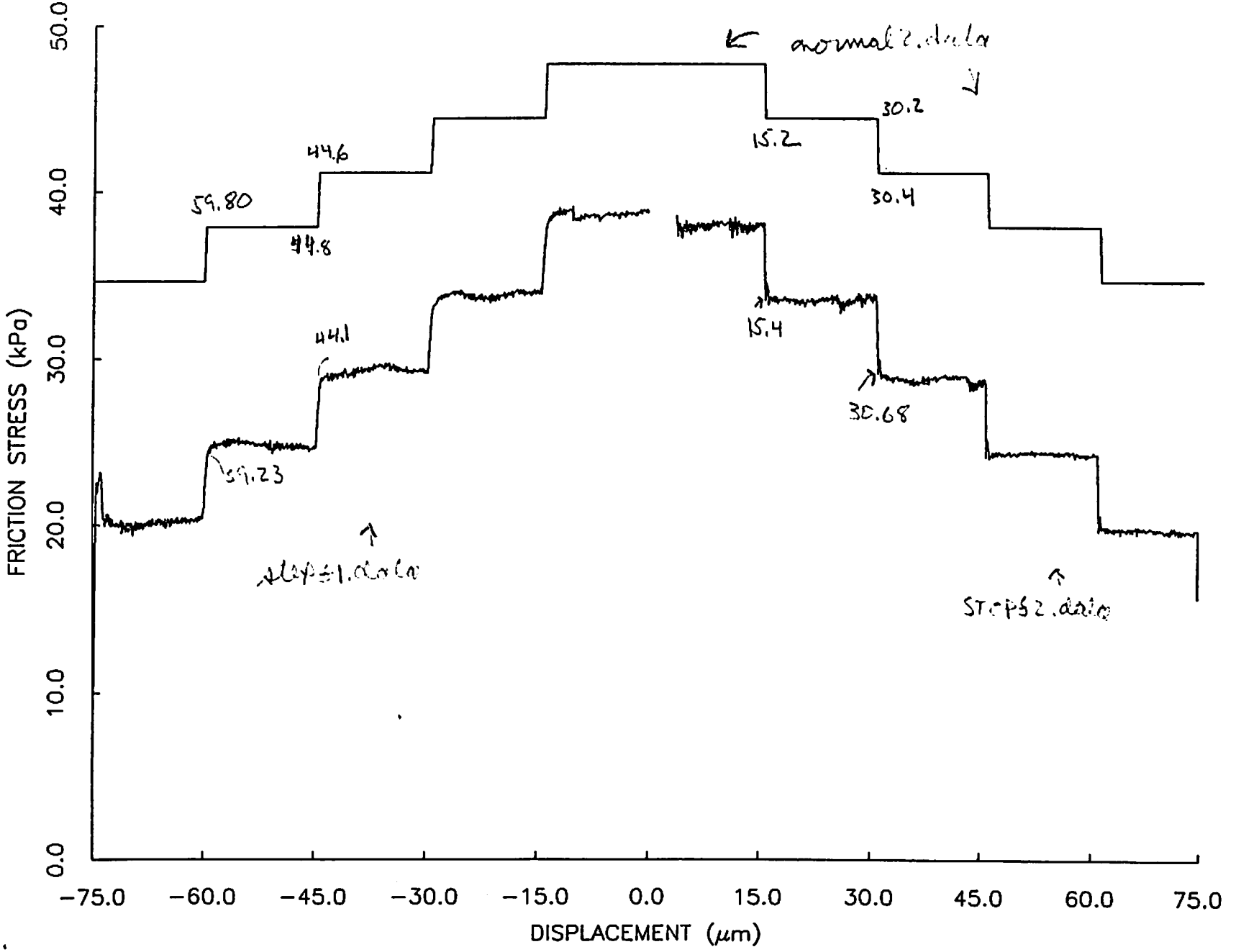

Fig. 10

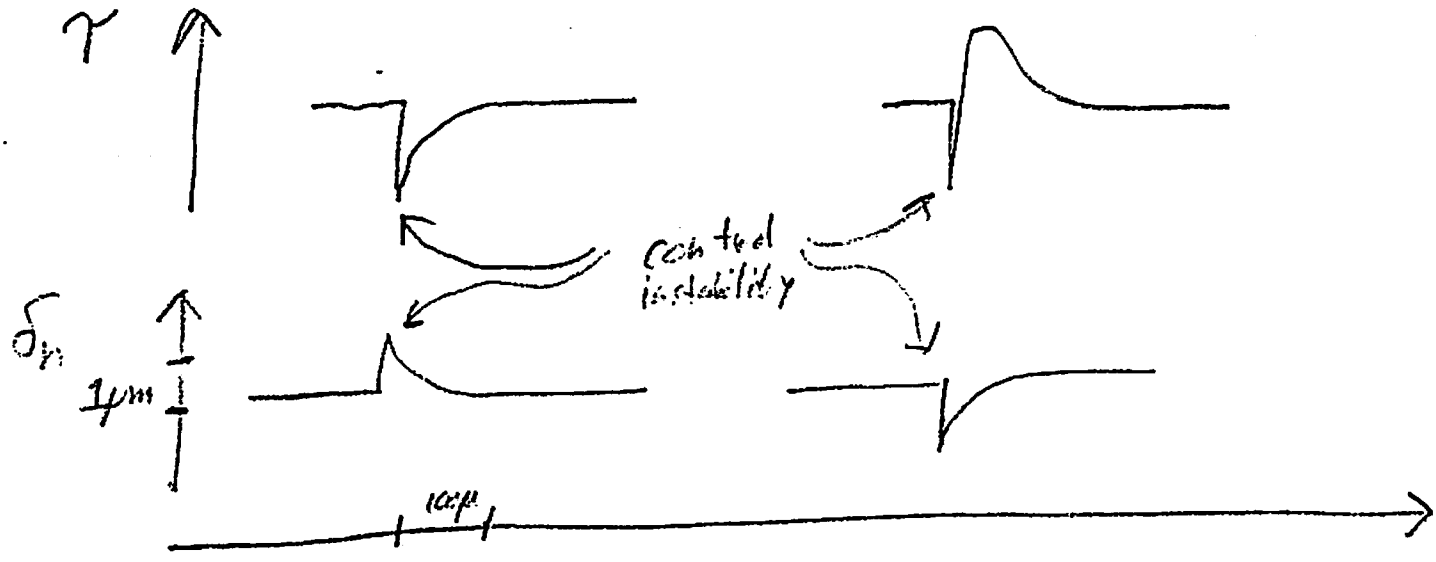

FIGURE 11

Normal Displ. & Shear stress when sample is disturbed.

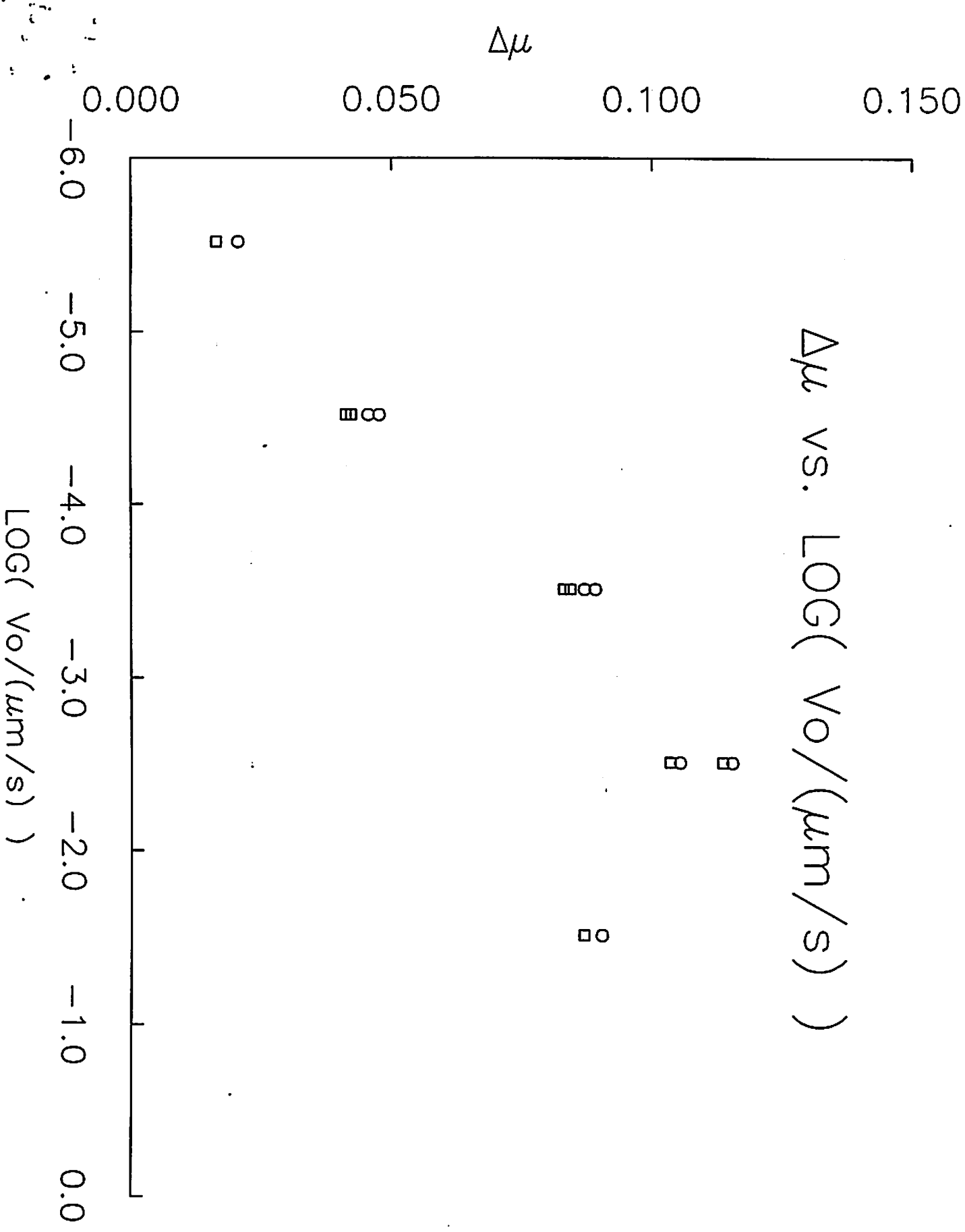
Δμ
0.000
0.050
0.100
0.150
−6.0
−5.0
−4.0
−3.0
−2.0
−1.0
0.0
LOG(Vo/(μm/s))
Δμ vs. LOG(Vo/(μm/s))

Fig. 12

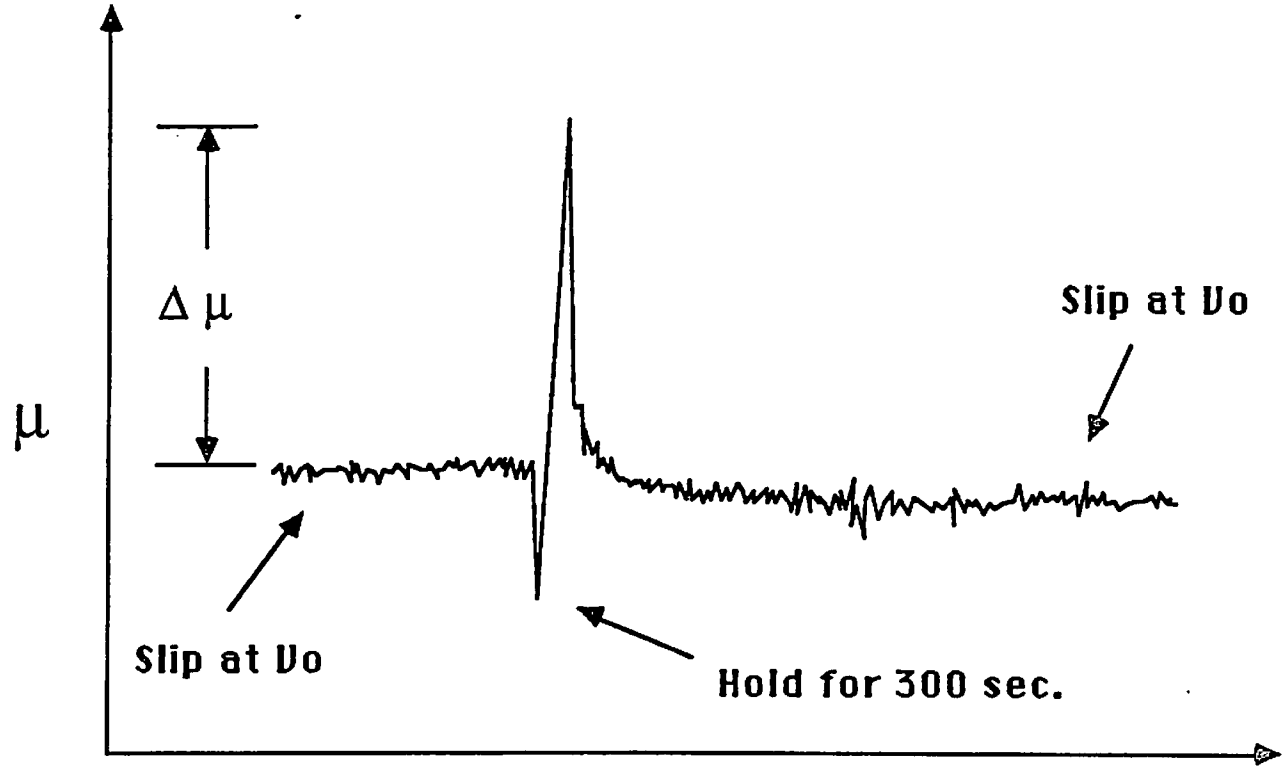

Fig. 12

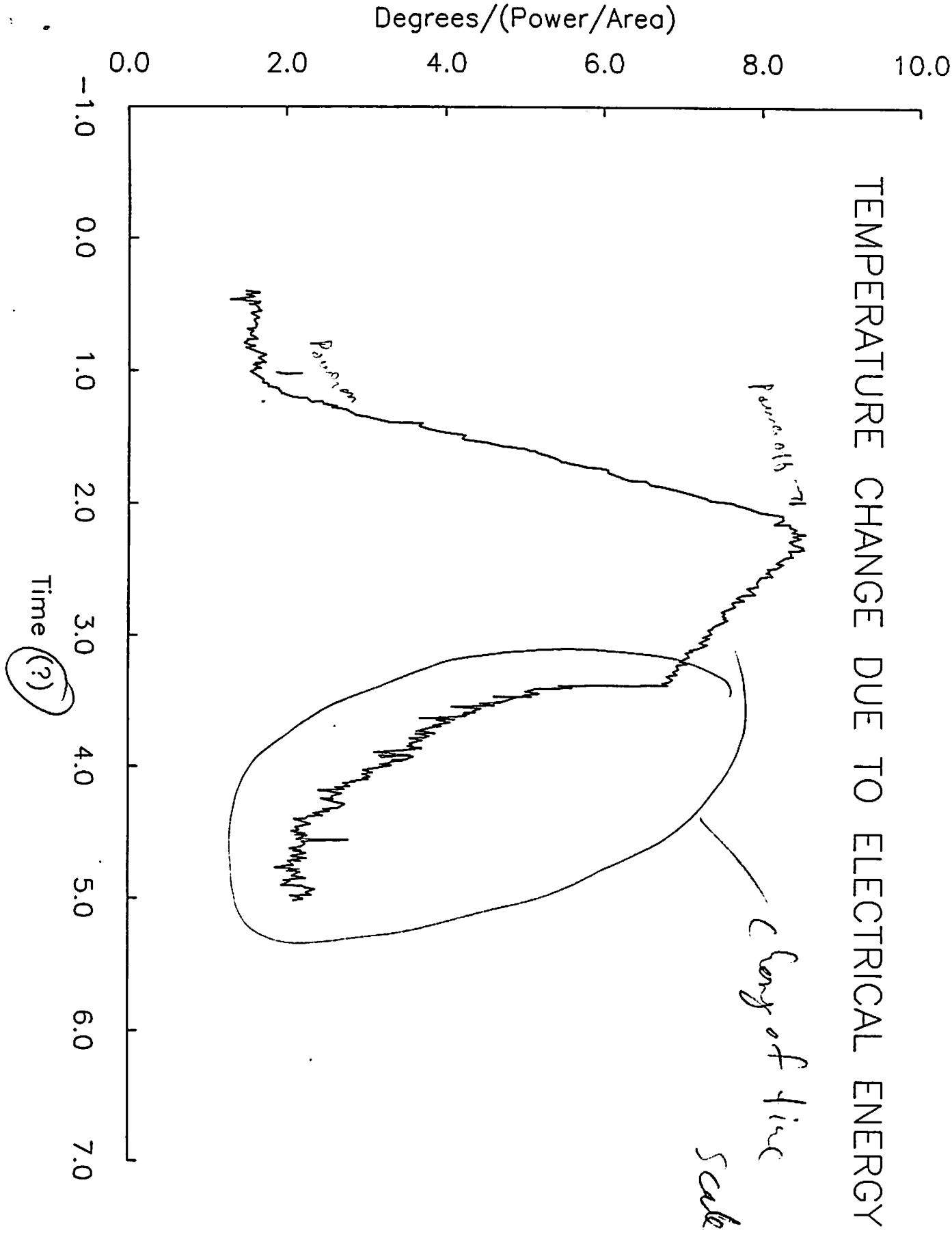
TEMPERATURE CHANGE DUE TO ELECTRICAL ENERGY
Degrees/(Power/Area)
0.0
2.0
4.0
6.0
8.0
10.0
-1.0
0.0
1.0
2.0
3.0
4.0
5.0
6.0
7.0
Time (?)
Power on
Power off
Change of time
Scale

Fig. 13

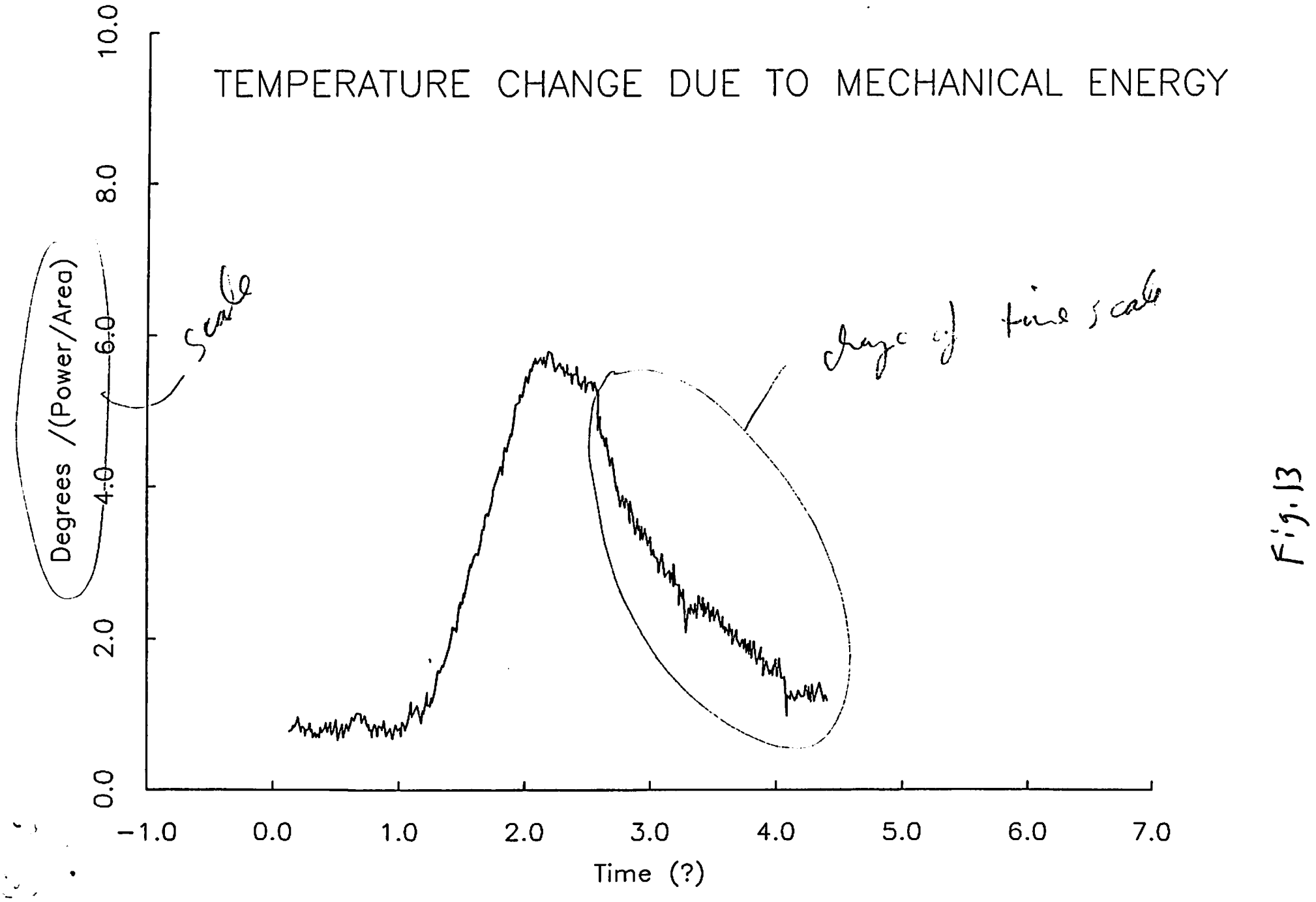
TEMPERATURE CHANGE DUE TO MECHANICAL ENERGY
Degrees /(Power/Area)
10.0
8.0
6.0
4.0
2.0
0.0
scale
range of time scale
−1.0
0.0
1.0
2.0
3.0
4.0
5.0
6.0
7.0
Time (?)

Fig. 13

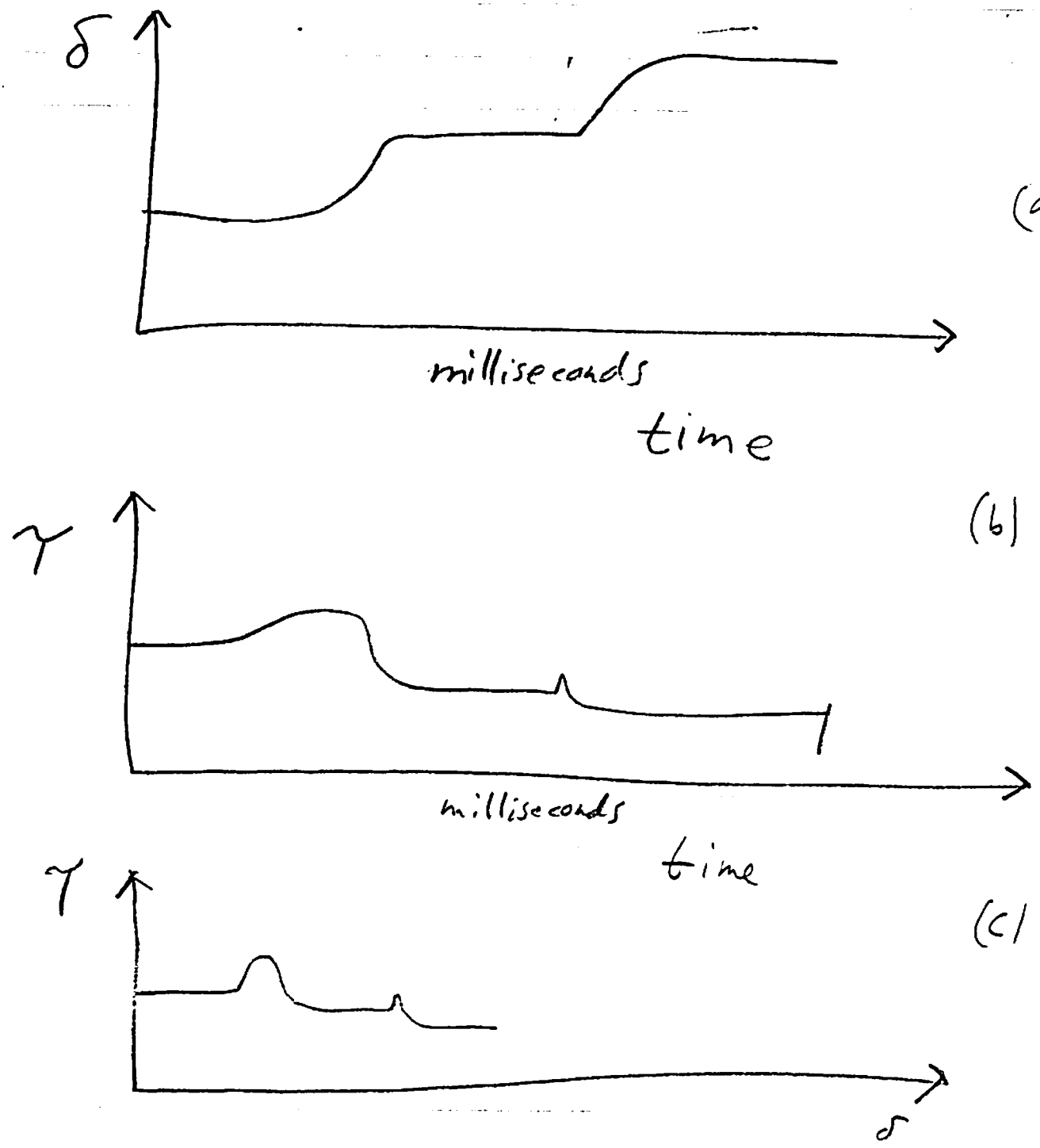

Figure 14

Dynamic Stick Slip test in sandwich shear.

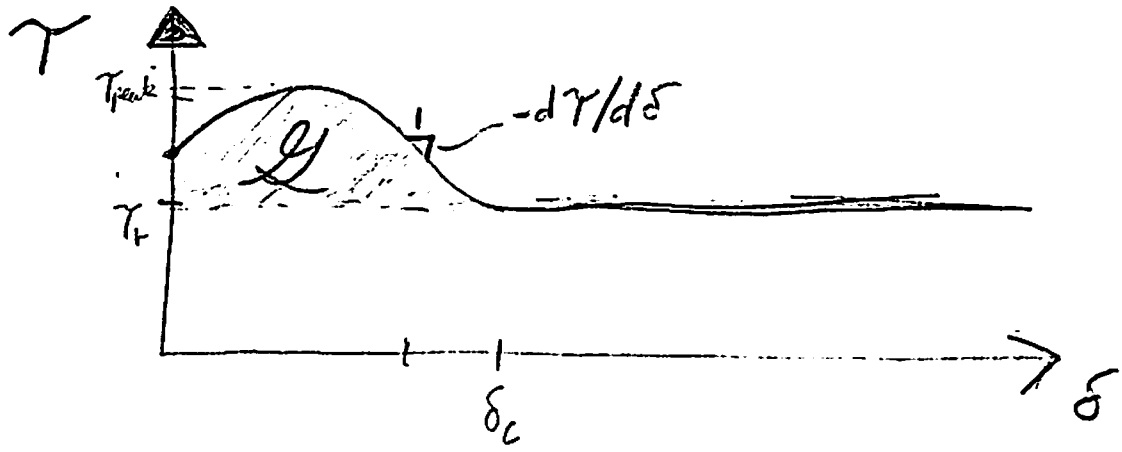

Slip weakening friction law,
FIGURE A1

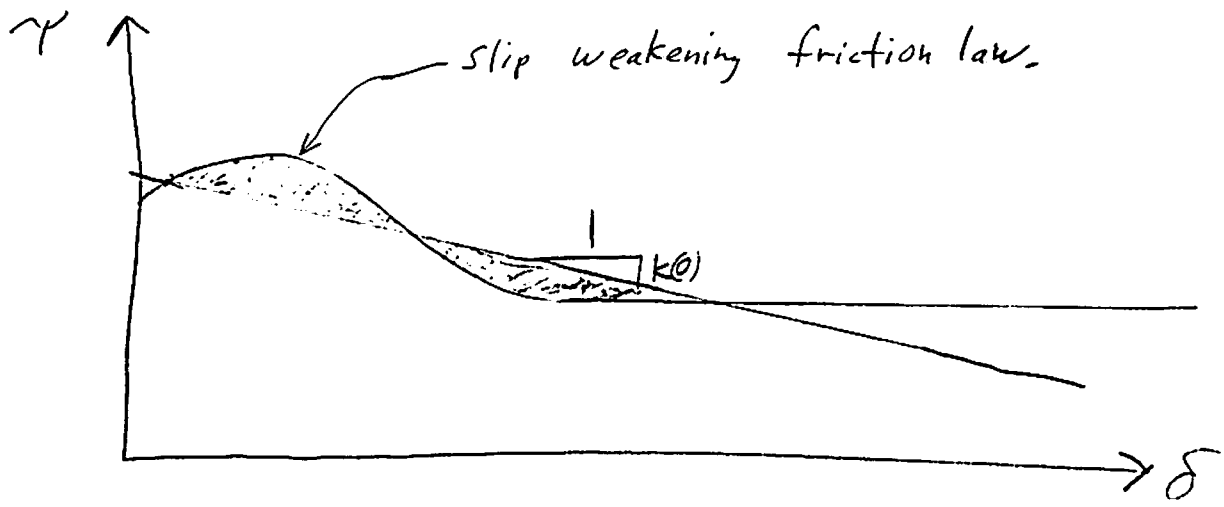

Equal shaded areas for fracture propagation.
Figure A2